

Graph-Theoretic Analysis of n -Replica Time Evolution in the Brownian Gaussian Unitary Ensemble

Tingfei Li,^{a,b} Cheng Peng,^{a,c} Jianghai Yu^a

^a*Kavli Institute for Theoretical Sciences (KITS), University of Chinese Academy of Sciences, Beijing 100190, China*

^b*Zhejiang Institute of Modern Physics, Zhejiang University, Hangzhou, 310027, P. R. China*

^c*Peng Huanwu Center for Fundamental Theory, Hefei, Anhui 230026, China*

E-mail: tfli@zju.edu.cn, yujianghai21@mails.ucas.ac.cn,
pengcheng@ucas.ac.cn

ABSTRACT: In this paper, we investigate the n -replica time evolution operator $\mathcal{U}_n(t) \equiv e^{\mathcal{L}_n t}$ for the Brownian Gaussian Unitary Ensemble (BGUE) using a graph-theoretic approach. We examine the moments of the generating operator \mathcal{L}_n , which governs the Euclidean time evolution within an auxiliary D^{2n} -dimensional Hilbert space, where D represents the dimension of the Hilbert space for the original system. Explicit representations for the cases of $n = 2$ and $n = 3$ are derived, emphasizing the role of graph categorization in simplifying calculations. Furthermore, we present a general approach to streamline the calculation of time evolution for arbitrary n , supported by a detailed example of $n = 4$. Our results demonstrate that the n -replica framework not only facilitates the evaluation of various observables but also provides valuable insights into the relationship between Brownian disordered systems and quantum information theory.

¹The author names are listed in alphabetical order.

Contents

1	Introduction	1
2	Analysis on Graphs	4
2.1	Notations of a Graph	5
2.2	Operating \mathcal{L}_n on an Individual Graph	7
3	Time Evolution for $n = 2$	9
3.1	Counting Graph Categories	9
3.2	Observables	12
4	Time Evolution for $n = 3$	13
4.1	Grouping Graphs into Categories	14
4.2	Operation of \mathcal{L}_3	18
4.3	Observables	19
5	General Cases	21
5.1	Example: $n = 4$	22
6	Discussions and Outlook	24
A	Expression of $\mathcal{U}_3(t)$	26

1 Introduction

Brownian disordered quantum systems have garnered significant interest across various fields, including many-body quantum chaos [1–3], quantum gravity [4, 5], and quantum information theory [4, 6–9]. Unlike systems with static (quenched) disorder, Brownian disorder is characterized by time-dependent randomness, allowing ensemble averaging to yield analytically tractable descriptions of non-equilibrium dynamics. A paradigmatic example is the Brownian Sachdev-Ye-Kitaev (SYK) model [10], which is significantly trackable than the regular SYK [11, 12]. This has led to its widespread use as a toy model for quantum gravity [13–16], quantum error correction (QEC) [17], out-of-time-ordered correlators (OTOCs) [18], and other fundamental aspects of quantum chaos [19–25].

Building on these developments, the recently proposed Brownian Gaussian Unitary Ensemble (BGUE) [9] offers an alternative setting to explore Brownian disorder in quantum systems. Unlike the standard Gaussian Unitary Ensemble (GUE), where the Hamiltonian

is randomly drawn but remains fixed in time, BGUE describes a system evolving under a time-dependent noisy Hamiltonian,

$$H_{ij}(t) = \eta_{ij}(t), \eta_{ij}(t) = \eta_{ij}^*(t) \in \mathbb{C}, \quad (1.1)$$

where $\eta_{ij}(t)$ are independent Brownian Gaussian random variables with vanishing mean and nonzero variance

$$\mathbb{E}(\eta_{ij}(t)) = 0, \quad \mathbb{E}(\eta_{ij}(t)\eta_{kl}(t')) = \frac{J}{D}\delta_{il}\delta_{jk}\delta(t-t'). \quad (1.2)$$

The time evolution in this setting can be regarded as the limiting case of an infinitely long piecewise stochastic evolution

$$U = e^{-iH_1t_1}e^{-iH_2t_2}\dots e^{-iH_nt_n}, \quad (1.3)$$

where each H_i is an independent realization of a GUE matrix. This model exhibits several remarkable properties, including rapid convergence to unitary k -designs [21, 22, 26–30], hyperfast scrambling and the emergence of temperature in de Sitter space [31]. Compared to conventional chaotic systems, the Brownian nature of BGUE ensures that ensemble-averaged quantities remain well-defined and analytically trackable, making it a powerful tool for exploring non-equilibrium dynamics.

One of the key motivations for studying BGUE lies in its connection to quantum information theory [32–40]. Random matrix models have long served as powerful tools for understanding quantum thermalization, entanglement growth, and operator spreading. In particular, BGUE has been shown to efficiently generate unitary designs, which play a central role in quantum information processing tasks such as classical shadow tomography [41] and quantum state reconstruction [9]. Furthermore, an essential feature of disordered quantum systems is their behavior under replica dynamics, a technique in which multiple copies of the system are introduced to probe statistical correlations. Many important quantum information measures—including entanglement entropy, operator norms, Rényi divergences, and multi-contour OTOC [42]—require analyzing multi-replica observables, making the study of n -replica time evolution in BGUE a crucial problem. However, existing studies have focused primarily on the cases $n = 1, 2$, leaving the general n -replica case largely unexplored. This serves as one of our motivations to study the general n -replica case and develop a systematic way to solve this question.

However, a fundamental challenge in extending the analysis to arbitrary n is the rapid growth in computational complexity. The effective time evolution of the n -replica

$$\mathcal{U}_n(t) \equiv \mathbb{E}(U^{\otimes n} \otimes U^{*\otimes n}) \equiv e^{\mathcal{L}_n t} \quad (1.4)$$

evolves within a Hilbert space of dimension D^{2n} , making direct matrix representations infeasible for large n . To simplify this question, we should note that the calculation of the

n -replica time evolution operator $\mathcal{U}_n(t)$ can be reduced to finding the general expression for the moments of \mathcal{L}_n , allowing for a straightforward expansion:

$$\mathcal{U}_n(t) = \sum_{r=0}^{\infty} \frac{(\mathcal{L}_n)^r t^r}{r!} . \quad (1.5)$$

We find that the linearly independent terms, which we refer to as “graphs”, that appear in the moments of \mathcal{L}_n are finite in number, allowing for a natural matrix representation. In the case of $n = 2$, the author of [9] categorized 24 individual graphs into 8 groups, reducing the matrix dimension from 24 to 8. However, as n increases, the number of individual graphs that emerge in the moments of \mathcal{L}_n grows rapidly (see Table 1), necessitating a systematic method to group these graphs into appropriate categories to achieve a significantly smaller-dimensional representation.

In this work, we develop a graph-theoretic framework for analyzing the time evolution of n -replica observables in BGUE. Our approach generalizes and extends the graph-based categorization introduced for $n = 2$, introducing a more structured notation that enables an algebraic treatment of replica dynamics. We demonstrate that the moments of \mathcal{L}_n can be mapped onto a finite set of graph categories, significantly reducing computational complexity.

For $n = 3$, we have 26 graph categories, so that \mathcal{L}_n is a 26-dimensional matrix. This enables us to obtain an explicit analytical expression for

$$e^{\mathcal{L}_n t} = \sum_{a=1}^{26} f_a(t) e^{-i\mathbf{E}t} \mathbf{F}_a , \quad (1.6)$$

where the analytical expressions of $f_a(t)$ are listed in Appendix A. Furthermore, we discuss the generalization of our framework to arbitrary n and present explicit results for $n = 4$.

Compared to representation-theoretic approaches, our graph-based method offers a lower-dimensional irreducible representation, reducing numerical computation time by handling a lower-dimensional matrix. Previous approaches, such as those in [43], relied on

$$[\mathcal{L}_n, V^{\otimes n} \otimes V^{*\otimes n}] = 0, \forall V \in U(D) , \quad (1.7)$$

which allows for the determination of eigenvalues and wavefunctions for \mathcal{L}_n by decomposing direct products of $SU(d)$ into irreducible representations. Moreover, these representations are constructed systematically using Young tableaux [44]. We will show the detailed result for $n = 2$ at the end of Sec. 3.

The graph representation also presents a straightforward way to compute the expectation values of observables. In cases where symmetries like (1.7) do not exist, the methodology discussed here can serve as a valuable toolbox. Beyond its application to BGUE, our framework has broader implications to other Brownian disordered systems, like random unitary circuit [45–49] and random tensor networks [50, 51]. The techniques developed here could provide new insights into the replica method in many-body quantum chaos, as well as potential applications to problems in wormholes and quantum gravity [52–55].

Structure of the Paper The remainder of this paper is structured as follows. In Sec. 2, we introduce the notation and graph-based formalism for representing the time evolution operator $\mathcal{U}_n(t)$. In Sec. 3, we apply our framework to the case $n = 2$ as a warm-up example, treated as a double check with the results from [9]. Sec. 4 extends this analysis to the non-trivial case $n = 3$, where we show how to find the graph categories and assign the graphs into them. In Sec. 5, we present a general algorithm for arbitrary n and illustrate its application to $n = 4$. Finally, in Sec. 6, we discuss potential future directions and broader implications of our findings.

2 Analysis on Graphs

In this section, we introduce a concise notation to represent arbitrary graphs, which facilitates the evaluation of graph contractions and enables a more transparent classification of graphs. We first establish the fundamental concepts, then discuss the inherent redundancies in this notation, and finally analyze the action of the group \mathcal{L}_n on individual graphs.

At first, we introduce some notations for the graph representation of \mathcal{U}_n and \mathcal{L}_n . We treat $\mathcal{U}_n, \mathcal{L}_n$ as a D^{2n} -dimensional matrix, with row and column indices labeled by two n -length lists: $\{I_1 J_1 I_2 J_2 \dots I_n J_n\}$ and $\{I'_1 J'_1 I'_2 J'_2 \dots I'_n J'_n\}$. We then adapt this to the graph representation (taking $n = 2$ as an example):

$$(\mathcal{U}_2(t))_{I_1 J_1 I_2 J_2; I'_1 J'_1 I'_2 J'_2} \equiv \mathbb{E} \left(U_{I_1 I'_1} U_{J_1 J'_1}^* U_{I_2 I'_2} U_{J_2 J'_2}^* \right) = \mathbb{E} \left[\begin{array}{c} \begin{array}{c} I_1 \text{---} \boxed{U} \text{---} I'_1 \\ J_1 \text{---} \boxed{U} \text{---} J'_1 \\ I_2 \text{---} \boxed{U} \text{---} I'_2 \\ J_2 \text{---} \boxed{U} \text{---} J'_2 \end{array} \end{array} \right] = \begin{array}{c} I_1 \text{---} \boxed{u_2} \text{---} I'_1 \\ J_1 \text{---} \boxed{u_2} \text{---} J'_1 \\ I_2 \text{---} \boxed{u_2} \text{---} I'_2 \\ J_2 \text{---} \boxed{u_2} \text{---} J'_2 \end{array} . \quad (2.1)$$

We label the indices in graphs using uppercase letters I, J, I', J' , where I/I' represent the left/right-hand side indices of a contour H , and J/J' denote the dual contour H^* . For simplicity, we label the contours (and dual contours) with lowercase letters i, j, k, l (and their corresponding bars $\bar{i}, \bar{j}, \bar{k}, \bar{l}$). Since we take $n = 2$, we can also represent \mathcal{U}_2 as

$$\mathcal{U}_2(t) = \begin{array}{c} \begin{array}{c} 1 \text{---} \boxed{u_2} \text{---} 1' \\ \bar{1} \text{---} \boxed{u_2} \text{---} \bar{1}' \\ 2 \text{---} \boxed{u_2} \text{---} 2' \\ \bar{2} \text{---} \boxed{u_2} \text{---} \bar{2}' \end{array} \end{array} \quad (2.2)$$

By a similar derivation as shown in [9], it is straightforward to obtain

$$\mathcal{L}_n = w\mathbb{I} + \frac{J}{D} \sum_{i\bar{j}}^n P_{i\bar{j}} - \frac{J}{D} \sum_{ij}^n (X_{ij} + X_{i\bar{j}}) \quad , \quad (2.3)$$

where J is the strength of noise, \mathbb{I} denotes identity operator. Other two kinds of operators are represented as below:

$$P_{i\bar{j}} = \begin{array}{c} i \\ \bar{j} \end{array} \text{---} \bigcap \quad , \quad X_{ij} = \begin{array}{c} i \\ j \end{array} \text{---} \bigwedge \quad , \quad (2.4)$$

where each line with two indices i, j at the endpoints of the graph represents a ‘‘propagator’’ between the sites on the contour and the dual contour, i.e., δ_{ij} . Other trivial propagators connecting sites on the same contour, which are represented as straight lines, are given by $\delta_{I_i I'_i}$ or $\delta_{J_i J'_i}$. Taking $n = 2$ as an example, we have

$$\begin{aligned}
(P_{1\bar{2}})_{I_1 J_1 I_2 J_2; I'_1 J'_1 I'_2 J'_2} &= \left[\begin{array}{c} 1 \\ \bar{1} \\ 2 \\ \bar{2} \end{array} \right]_{I_1 J_1 I_2 J_2; I'_1 J'_1 I'_2 J'_2} = \delta_{I_1 J_2} \delta_{I'_1 J'_2} \delta_{J_1 J'_1} \delta_{I_2 I'_2} , \\
(X_{12})_{I_1 J_1 I_2 J_2; I'_1 J'_1 I'_2 J'_2} &= \left[\begin{array}{c} 1 \\ \bar{1} \\ 2 \\ \bar{2} \end{array} \right]_{I_1 J_1 I_2 J_2; I'_1 J'_1 I'_2 J'_2} = \delta_{I_1 I'_2} \delta_{I_2 I'_1} \delta_{J_1 J'_1} \delta_{J_2 J'_2} . \quad (2.5)
\end{aligned}$$

And w in (2.3) is a factor that carries the indices of a graph

$$w_{I_1 J_1 I_2 J_2 \dots I_n J_n} = -i \sum_{j=1}^n (E_{I_j} - E_{J_j}) - nJ, \quad i = \sqrt{-1} . \quad (2.6)$$

Notice that the factor $w_{I_1 J_1 I_2 J_2 \dots I_n J_n}$ commutes with all of the terms in \mathcal{L}_n . For instance,

$$w_{I_1 J_1 I_2 J_2 \dots I_n J_n} (P_{a\bar{b}})_{I_1 J_1 I_2 J_2 \dots I_n J_n; I'_1 J'_1 I'_2 J'_2 \dots I'_n J'_n} = (P_{a\bar{b}})_{I_1 J_1 I_2 J_2 \dots I_n J_n; I'_1 J'_1 I'_2 J'_2 \dots I'_n J'_n} w_{I'_1 J'_1 I'_2 J'_2 \dots I'_n J'_n} . \quad (2.7)$$

Thus, from now on, we can treat w as an ordinary constant and simply write it as w . For later use, we define the spectrum factor

$$E_{I_1 J_1 I_2 J_2 \dots I_n J_n} = -i \sum_{j=1}^n (E_{I_j} - E_{J_j}) . \quad (2.8)$$

Since $w = E - nJ\mathbb{I}$, the factor $E_{I_1 J_1 I_2 J_2 \dots I_n J_n}$ also commutes with all terms in \mathcal{L}_n .

2.1 Notations of a Graph

In this work, we employ a concise notation $F = \prod_{i=1}^p c_{a_i \bar{b}_i} c[\sigma]$ to represent an arbitrary graph. Here, $0 \leq p \leq n$ denotes the number of paired vertices, and $\sigma \equiv \sigma_H \otimes \sigma_{H^*} \in S_n \otimes S_n$ encodes the permutation acting on the indices appearing on the right-hand side of the graph. The element of a D^{2n} -dimensional matrix $F_{I_1 J_1 I_2 J_2 \dots I_n J_n; I'_1 J'_1 I'_2 J'_2 \dots I'_n J'_n}$ would be:

$$\left(\prod_{i=1}^p c_{a_i \bar{b}_i} c[\sigma] \right)_{\{I J\}; \{I' J'\}} = \prod_{i \notin \{a\}, \bar{j} \notin \{\bar{b}\}} \delta_{I_i I'_{\sigma_1(i)}} \delta_{J_{\bar{j}} J'_{\sigma(\bar{j})}} \prod_{i=1}^p \delta_{I_{a_i} J_{\bar{b}_i}} \delta_{I'_{\sigma_1(a_i)} J'_{\sigma_2(\bar{b}_i)}} . \quad (2.9)$$

Here, $c[\sigma]$ is the permutation on the contour labels on the right-hand side, $c_{i\bar{j}}$ represents the pair between the left sites i, \bar{j} and the right sites $\sigma(i)', \sigma(\bar{j})'$. To make the complicated

notations clear, we can take a simple example $c_{1\bar{1}}c[X_{12} \otimes X_{\bar{1}\bar{2}}] = \delta_{I_1 J_1} \delta_{I'_2 J'_2} \delta_{I_2 J'_1} \delta_{J_2 J'_1}$ and show how the graphs work as follows:

$$\begin{array}{ccccccc}
\begin{array}{cc} 1 \bullet & \bullet 1' \\ \bar{1} \circ & \circ \bar{1}' \end{array} & & \begin{array}{cc} 1 \bullet & \bullet 2' \\ \bar{1} \circ & \circ \bar{2}' \end{array} & \xrightarrow{c[X_{12} \otimes X_{\bar{1}\bar{2}}]} & \begin{array}{cc} 1 \bullet & \bullet 2' \\ \bar{1} \circ & \circ \bar{2}' \end{array} & \xrightarrow{c_{1\bar{1}}} & \begin{array}{cc} 1 \bullet & \bullet 2' \\ \bar{1} \circ & \circ \bar{2}' \end{array} \\
\begin{array}{cc} 2 \bullet & \bullet 2' \\ \bar{2} \circ & \circ \bar{2}' \end{array} & & \begin{array}{cc} 2 \bullet & \bullet 1' \\ \bar{2} \circ & \circ \bar{1}' \end{array} & & \begin{array}{cc} 2 \bullet & \bullet 1' \\ \bar{2} \circ & \circ \bar{1}' \end{array} & & \begin{array}{cc} 1 \bullet & \bullet 1' \\ \bar{1} \circ & \circ \bar{1}' \end{array} \\
& & & & & & = & \begin{array}{cc} 1 \bullet & \bullet 1' \\ \bar{1} \circ & \circ \bar{1}' \end{array} \cdot
\end{array} \tag{2.10}$$

The filled dots are the sites on the contour H and the hollow circles are those on the dual contour H^* . And we can directly find how the swapping and connecting operations work in the first two steps. The graph is finally denoted as the R.H.S. of (2.10).

The notations presented in (2.9) for the graphs make it much easier to calculate the contraction (product) of two graphs and study the action of \mathcal{L}_n on a certain graph, as we will see later in this section.

Symmetries of a Graph Before examining the action of $P_{i\bar{j}}$ and $X_{ij}, X_{\bar{i}\bar{j}}$ on a graph F , we note that the notations presented above have some redundancy. For a graph $F = \prod_{i=1}^p c_{a_i \bar{b}_i} c[\sigma]$, the vertices for each connected pair (a_i, \bar{b}_i) are identical. To simplify it, we define the action of a permutation on the graph as

$$\sigma' * F \equiv \sigma' \left(\prod_{i=1}^p c_{a_i \bar{b}_i} \right) c[\sigma \sigma'] = \prod_{i=1}^p c_{\sigma'_1(a_i) \sigma'_2(\bar{b}_i)} c[\sigma \sigma'] . \tag{2.11}$$

If a permutation $\sigma' = \sigma'_H \otimes \sigma'_{H^*}$ is an element of the group $G_n(\mathbf{a}, \bar{\mathbf{b}})$ generated by $\{X_{a_i a_j} \otimes X_{\bar{b}_i \bar{b}_j}\}_{i,j=1,2,\dots,p}$, then its action is trivial: $\sigma' * F = \prod_{i=1}^p c_{a_i \bar{b}_i} c[\sigma \sigma'] = F$. It can be observed that $G_n(\mathbf{a}, \bar{\mathbf{b}})$ resembles the gauge group in quantum field theory and is isomorphic to the permutation group S_p .

n	N_n	# Graph Categories
1	2	2
2	24	8
3	720	26
4	40320	/
5	3628800	/

Table 1. Number of individual graphs and graph categories.

Number of Individual Graphs For a given n , the task is to count the number of individual graphs N_n generated by \mathcal{L}_n . A simple counting yields:

$$N_1 = 2, \quad N_2 = 24.$$

For general n , using $|G_n(\mathbf{a}, \bar{\mathbf{b}})| = p!$ and $|S_n \otimes S_n| = (n!)^2$, we have

$$N_n = \sum_{\mathbf{a}, \bar{\mathbf{b}}} \frac{|S_n \otimes S_n|}{|G_n(\mathbf{a}, \bar{\mathbf{b}})|} = \sum_{p=0}^n \binom{n}{p}^2 p! \frac{(n!)^2}{p!} = \sum_{p=0}^n \left(n! \binom{n}{p} \right)^2 \equiv \sum_{p=0}^n N_{n,p} . \quad (2.12)$$

One can utilize the individual graphs as a basis, then $\mathcal{L}_n \mathbf{F}_i = \sum_{j=1}^{N_n} \widetilde{M}_{ji} \mathbf{F}_j$. However, as indicated in (2.12), the dimension of \widetilde{M} grows too quickly with n . A clever approach is to group these individual graphs into categories $\mathbf{F}_\alpha = \sum_{i=1}^{N_n} \mathbf{F}_{\alpha,i}$ such that

$$\mathcal{L}_n \mathbf{F}_\alpha = \sum_{\beta=1}^{N_n^{\text{ca}}} M_{\beta\alpha} \mathbf{F}_\beta . \quad (2.13)$$

In this paper, we further require that $\mathbf{F}_\alpha \cap \mathbf{F}_\beta = \emptyset$ for all $\alpha \neq \beta$. The dimension of the transfer matrix M , denoted as N_n^{ca} , can be significantly smaller than N_n , as illustrated in Table 1.

2.2 Operating \mathcal{L}_n on an Individual Graph

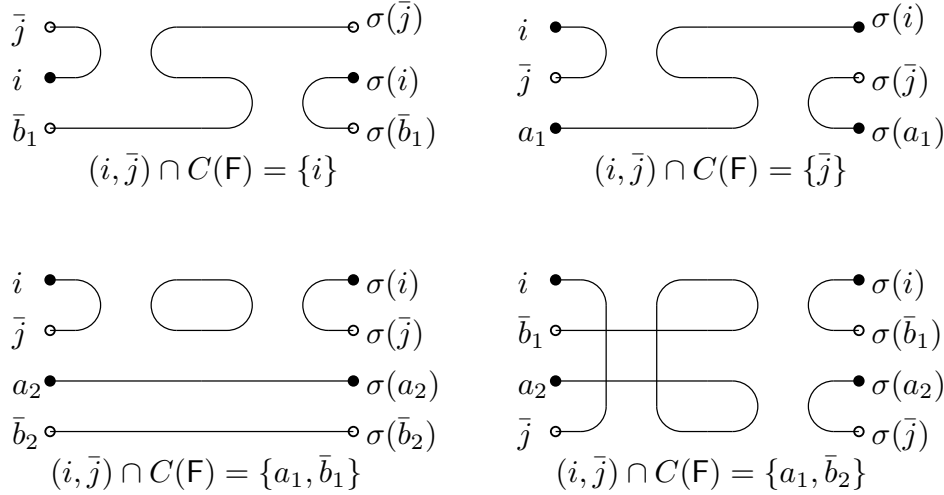


Figure 1. Four non-trivial cases of $P_{i\bar{j}}\mathbf{F}$.

Since \mathcal{L}_n consists of $P_{i\bar{j}}$ and $X_{ij}, X_{\bar{i}\bar{j}}$, we first evaluate their action on an individual graph $\mathbf{F} = \prod_{i=1}^p c_{a_i \bar{b}_i} c[\sigma]$. We denote the set of paired sites as $C(\mathbf{F}) = \{(a_i, \bar{b}_i)\}_{i=1}^p$. For later reference, we also define the set of all possible paired sites between different contours as \mathcal{C} and those on the same contour as \mathcal{E} and $\bar{\mathcal{E}}$, respectively:

$$\mathcal{C} \equiv \{(i, \bar{j})\}_{1 \leq i, \bar{j} \leq n}, \mathcal{E} \equiv \{(i, j)\}_{1 \leq i < j \leq n}, \bar{\mathcal{E}} \equiv \{(\bar{i}, \bar{j})\}_{1 \leq \bar{i} < \bar{j} \leq n} . \quad (2.14)$$

Operation of $P_{i\bar{j}}$ There are five cases:

$$P_{i\bar{j}}\mathbf{F} = \begin{cases} c_{i\bar{j}}\mathbf{F}, & \text{if } (i, \bar{j}) \cap C(\mathbf{F}) = \emptyset \\ X_{\bar{j}\bar{b}_1} * \mathbf{F}, & \text{if } (i, \bar{j}) \cap C(\mathbf{F}) = \{a_1\} \\ X_{ia_1} * \mathbf{F}, & \text{if } (i, \bar{j}) \cap C(\mathbf{F}) = \{\bar{b}_1\} \\ D\mathbf{F}, & \text{if } (i, \bar{j}) \cap C(\mathbf{F}) = \{a_1, \bar{b}_1\} \\ X_{a_1a_2} * \mathbf{F} = X_{\bar{b}_1\bar{b}_2} * \mathbf{F}, & \text{if } (i, \bar{j}) \cap C(\mathbf{F}) = \{a_1, \bar{b}_2\} \end{cases}. \quad (2.15)$$

Since the first case is trivial, we illustrate the other four cases in Figure 1.

Operation of $X_{ij}, X_{i\bar{j}}$ There are five cases depending on the result of $(i, j) \cap C(\mathbf{F})$. We depict two nontrivial cases in Figure 2. It is observed that we always have

$$X_{ij}\mathbf{F} = X_{ij} * \mathbf{F},$$

and the action of $X_{i\bar{j}}$ is given by

$$X_{i\bar{j}}\mathbf{F} = X_{i\bar{j}} * \mathbf{F}.$$

Operation of \mathcal{L}_n Next, we can study the operation of \mathcal{L}_n . Notice that we have the condition $\bar{u} \cap C[\mathbf{F}] = \emptyset$. Hence the permutations X_u and $X_{\bar{u}}$ act trivially on $C(\mathbf{F})$. Thus, we ultimately find a simple relation

$$\mathcal{L}_n\mathbf{F} = (w + |C[\mathbf{F}]|J)\mathbf{F} + \frac{J}{D} \sum_{u \cap C[\mathbf{F}] = \emptyset} c_u \mathbf{F} - \frac{J}{D} \sum_{u \cap C[\mathbf{F}] = \emptyset} \mathbf{F}[\sigma X_u] - \frac{J}{D} \sum_{\bar{u} \cap C[\mathbf{F}] = \emptyset} \mathbf{F}[\sigma X_{\bar{u}}] \quad (2.16)$$

where $|C[\mathbf{F}]|$ counts the number of pairs, and $\mathbf{F}[\sigma\sigma'] \equiv \prod_{i=1}^p c_{a_i\bar{b}_i} c[\sigma\sigma']$. The definitions of u and \bar{u} are encoded in the summation expressions. For example, in the term $\sum_{u \cap C[\mathbf{F}] = \emptyset} c_u \mathbf{F}$, u can be considered as a pair in \mathcal{C} that is excluded by $C(\mathbf{F})$. Meanwhile, in the term $\sum_{u \cap C[\mathbf{F}] = \emptyset} \mathbf{F}[\sigma X_u]$, u can be regarded as an element of \mathcal{E} that is excluded by $C(\mathbf{F})$. Here we choose the set of u to meet those conditions of $u \cap C[\mathbf{F}] = \emptyset$ from all the summations, which requires flattening $C(\mathbf{F})$ into a list of site labels and find those u that are available. For example, taking $u = \{(1, \bar{1})\}$, $C(\mathbf{F}) = \{(1, \bar{2}), (2, \bar{3})\}$, then

$$u \cap C(\mathbf{F}) = \{1, \bar{1}\} \cap \{1, \bar{2}, 2, \bar{3}\} = \{1\} \neq \emptyset, \quad (2.17)$$

which shows that $u = \{(1, \bar{1})\}$ is not available.

We always define three graph categories, as they play a crucial role in the definition of \mathcal{L}_n :

$$\mathbf{F}_0 \equiv c[I], \mathbf{F}_1 \equiv \sum_u c_u c[I], \mathbf{F}_{0, X+\bar{X}} \equiv \sum_e c[X_e] + \sum_{\bar{e}} c[X_{\bar{e}}]. \quad (2.18)$$

Then we apply \mathcal{L}_n to the three initial categories and their descendants until a complete basis is obtained. After that, we obtain the expression for the transfer matrix M in (2.13), which allows us to solve $\mathcal{U}_n(t)$ using (1.5). We will illustrate the basic idea with examples for $n = 2$ and $n = 3$ in the next two sections.

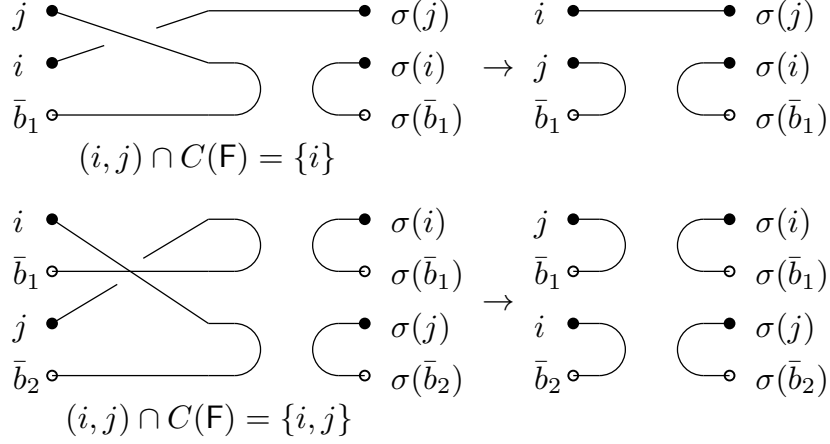


Figure 2. Two non-trivial cases of $X_{ij}F$.

3 Time Evolution for $n = 2$

As a warm-up, we consider $n = 2$, which gives us four sites: $\{1, \bar{1}, 2, \bar{2}\}$. The permutation group is $S_2 \otimes S_2$, where $S_2 = \{I, X_{12}\}$. Then

$$\begin{aligned} \mathcal{C} &= \{(1, \bar{1}), (1, \bar{2}), (2, \bar{1}), (2, \bar{2})\} , \\ \mathcal{E} &= \{(1, 2)\}, \bar{\mathcal{E}} = \{(\bar{1}, \bar{2})\} . \end{aligned} \quad (3.1)$$

So we have

$$\mathcal{L}_2 = w\mathbb{I} + \frac{J}{D}(P_{1\bar{1}} + P_{2\bar{2}} + P_{1\bar{2}} + P_{2\bar{1}}) - \frac{J}{D}(X_{12} + X_{\bar{1}\bar{2}}) . \quad (3.2)$$

The number of individual graphs is 24, while the number of operators $(P_{i\bar{j}}, X_{ij}, X_{\bar{i}\bar{j}})$ is 6. Therefore, in principle, one needs to calculate $6 \times 24 = 168$ graph contractions when calculating M as defined earlier. Fortunately, (2.16) enables us to perform a simple algebraic calculation without drawing any graphs.

3.1 Counting Graph Categories

As we have discussed earlier, we will find the appropriate graph groups by applying \mathcal{L}_n to the three initial categories $F_0, F_1, F_{0, X+\bar{X}}$ and their descendants until no new graph category is generated. In the case of $n = 2$, we will perform \mathcal{L}_2 on the initial sets as follows.

\mathcal{L}_2 acts on $F_0, F_1, F_{0, X+\bar{X}}$

- $\mathcal{L}_2 F_0$: The operation of \mathcal{L}_2 on F_0 is trivial, since F_0 is a trivial set

$$\mathcal{L}_2 F_0 = wF_0 + \frac{J}{D}F_1 - \frac{J}{D}F_{0, X+\bar{X}} . \quad (3.3)$$

- $\mathcal{L}_2\mathbf{F}_1$: By definition we have

$$\mathcal{L}_2\mathbf{F}_1 = (w + J)\mathbf{F}_1 + \frac{J}{D} \sum_{u \neq v} c_u c_v c[I] - \frac{J}{D} \left(\sum_{e \cap u = \emptyset} c_u c[X_e] + \sum_{\bar{e} \cap u = \emptyset} c_u c[X_{\bar{e}}] \right). \quad (3.4)$$

Notice that the condition $e \cap u = \emptyset$, where $e \in \mathcal{E}$ and $u \in \mathcal{C}$, cannot be satisfied for $n = 2$. This is an important fact that simplifies the calculations for $n = 2$. Therefore, we have

$$\mathcal{L}_2\mathbf{F}_1 = (w + J)\mathbf{F}_1 + \frac{2J}{D}\mathbf{F}_2, \quad (3.5)$$

where we have defined

$$\mathbf{F}_2 \equiv \frac{1}{2!} \sum_{u \neq v} c_u c_v c[I] = c_{1\bar{1}} c_{2\bar{2}} c[I] + c_{1\bar{2}} c_{2\bar{1}} c[I]. \quad (3.6)$$

- $\mathcal{L}_2\mathbf{F}_{0, X+\bar{X}}$: It is direct to obtain

$$\begin{aligned} \mathcal{L}_2\mathbf{F}_{0, X+\bar{X}} &= w\mathbf{F}_{0, X+\bar{X}} + \frac{J}{D} \sum_u c_u \mathbf{F}_{0, X+\bar{X}} \\ &\quad - \frac{J}{D} \sum_{e, u} (c[X_e X_u] + c[X_{\bar{e}} X_u] + c[X_e X_{\bar{u}}] + c[X_{\bar{e}} X_{\bar{u}}]), \end{aligned} \quad (3.7)$$

then we can define $\mathbf{F}_{1, X+\bar{X}} \equiv \sum_u c_u \mathbf{F}_{0, X+\bar{X}}$. Notice that

$$\sum_{e, u} (c[X_e X_u] + c[X_{\bar{e}} X_u] + c[X_e X_{\bar{u}}] + c[X_{\bar{e}} X_{\bar{u}}]) = 2c[I] + 2c[X_{12} X_{\bar{1}\bar{2}}]. \quad (3.8)$$

So we can define $\mathbf{F}_{0, X\bar{X}} \equiv c[X_{12} X_{\bar{1}\bar{2}}]$, then

$$\mathcal{L}_2\mathbf{F}_{0, X+\bar{X}} = w\mathbf{F}_{0, X+\bar{X}} + \frac{J}{D}\mathbf{F}_{1, X+\bar{X}} - \frac{2J}{D}(\mathbf{F}_0 + \mathbf{F}_{0, X\bar{X}}). \quad (3.9)$$

We find that three new graph categories, $\mathbf{F}_2, \mathbf{F}_{1, X+\bar{X}}, \mathbf{F}_{0, X\bar{X}}$, emerge after applying \mathcal{L}_2 on initial sets, which is the first order calculations. Next, we consider the second order, which means the operation of \mathcal{L}_2 on these new categories. For clarity, we restate the definitions here

$$\mathbf{F}_2 = c_{1\bar{1}} c_{2\bar{2}} c[I] + c_{1\bar{2}} c_{2\bar{1}} c[I], \quad (3.10)$$

$$\mathbf{F}_{1, X+\bar{X}} = \sum_u c_u \mathbf{F}_{0, X+\bar{X}}, \quad (3.11)$$

$$\mathbf{F}_{0, X\bar{X}} = c[X_{12} X_{\bar{1}\bar{2}}]. \quad (3.12)$$

\mathcal{L}_2 acts on $F_2, F_{1, X+\bar{X}}, F_{0, X\bar{X}}$

- $\mathcal{L}_2 F_2$: Notice that only the first term in (2.16) survives. The operation of \mathcal{L}_2 on F_2 is straightforward to obtain

$$\mathcal{L}_2 F_2 = (w + 2J) F_2 . \quad (3.13)$$

- $\mathcal{L}_2 F_{1, X+\bar{X}}$: Using (2.16), we have

$$\mathcal{L}_2 F_{1, X+\bar{X}} = (w + J) F_{1, X+\bar{X}} + \frac{J}{D} \left(\sum_e \sum_{g \cap u = \emptyset} c_g c_u c[X_e] + (e \leftrightarrow \bar{e}) \right) , \quad (3.14)$$

so we can define

$$F_{2, X+\bar{X}} \equiv \frac{1}{4} \sum_e \sum_{g \cap u = \emptyset} c_g c_u c[X_e] + (e \leftrightarrow \bar{e}) = c_{1\bar{1}} c_{2\bar{2}} c[X_{12}] + c_{1\bar{2}} c_{2\bar{1}} c[X_{12}] . \quad (3.15)$$

Finally, we have

$$\mathcal{L}_2 F_{1, X+\bar{X}} = (w + J) F_{1, X+\bar{X}} + \frac{4J}{D} F_{2, X+\bar{X}} . \quad (3.16)$$

- $\mathcal{L}_2 F_{0, X\bar{X}}$: Using (2.16), we have

$$\begin{aligned} \mathcal{L}_2 F_{0, X\bar{X}} &= w F_{0, X\bar{X}} + \frac{J}{D} \sum_u c_u c[X_{12} X_{\bar{1}\bar{2}}] - \frac{J}{D} \left(\sum_u c[X_{12} X_{\bar{1}\bar{2}} X_u] + \sum_u c[X_{12} X_{\bar{1}\bar{2}} X_{\bar{u}}] \right) \\ &= w F_{0, X\bar{X}} + \frac{J}{D} F_{1, X\bar{X}} - \frac{J}{D} (c[X_{\bar{1}\bar{2}}] + c[X_{12}]) \\ &= w F_{0, X\bar{X}} + \frac{J}{D} F_{1, X\bar{X}} - \frac{J}{D} F_{0, X+\bar{X}} \end{aligned} \quad (3.17)$$

where we have used $X_u = \{X_{12}\}$, so that $X_{12} X_{\bar{1}\bar{2}} X_u = X_{\bar{1}\bar{2}}, X_{12} X_{\bar{1}\bar{2}} X_{\bar{u}} = X_{12}$.

Here, we find two new graph categories, $F_{2, X+\bar{X}}$ and $F_{1, X\bar{X}}$. We will then study the third order calculations by operating \mathcal{L}_2 on these categories

$$F_{2, X+\bar{X}} = c_{1\bar{1}} c_{2\bar{2}} c[X_{12}] + c_{1\bar{2}} c_{2\bar{1}} c[X_{12}] , \quad (3.18)$$

$$F_{1, X\bar{X}} = \sum_u c_u c[X_{12} X_{\bar{1}\bar{2}}] . \quad (3.19)$$

\mathcal{L}_2 acts on $F_{2, X+\bar{X}}, F_{1, X\bar{X}}$ The calculations are straightforward by using (2.16)

- $\mathcal{L}_2 F_{2, X+\bar{X}}$:

$$\mathcal{L}_2 F_{2, X+\bar{X}} = (w + 2J) F_{2, X+\bar{X}} . \quad (3.20)$$

Rank r	New Categories	#F
1	$F_0, F_1, F_{0, X+\bar{X}}$	$1+4+2=7$
2	$F_2, F_{1, X+\bar{X}}, F_{0, X\bar{X}}$	$2+8+1=11$
3	$F_{2, X+\bar{X}}, F_{1, X\bar{X}}$	$2+4=6$
4	\emptyset	0

Table 2. 8 categories for $n = 2$.

- $\mathcal{L}_2 F_{1, X\bar{X}}$:

$$\begin{aligned}
\mathcal{L}_2 F_{1, X\bar{X}} &= (w + J) F_{1, X\bar{X}} + \frac{J}{D} \sum_{v \cap u = \emptyset} \sum_u c_v c_u c[X_{12} X_{\bar{1}\bar{2}}] \\
&= (w + J) F_{1, X\bar{X}} + \frac{J}{D} \sum_{v \cap u = \emptyset} \sum_u c_v c_u c[I] \\
&= (w + J) F_{1, X\bar{X}} + \frac{2J}{D} F_2,
\end{aligned} \tag{3.21}$$

where we have used the gauge redundancy: $c_u c_v c[\sigma X_{12} X_{\bar{1}\bar{2}}] = c_u c_v c[\sigma]$.

So far, we find that no new categories emerge. In summary, we list the total of 8 categories in Table 2.

3.2 Observables

Comparing with the categories in [9], we can choose

$$\{F_a\}_{a=1}^8 = \{F_{0,I}, F_{1,I}, F_{0, X+\bar{X}}, F_{1, X+\bar{X}}, F_{2,I}, F_{0, X\bar{X}}, F_{2, X\bar{X}}, F_{1, X\bar{X}}\}, \tag{3.22}$$

then we obtain the matrix representation of \mathcal{L}_2 :

$$M = \begin{pmatrix} w & 0 & -\frac{2J}{D} & 0 & 0 & 0 & 0 & 0 \\ \frac{J}{D} & J+w & 0 & 0 & 0 & 0 & 0 & 0 \\ -\frac{J}{D} & 0 & w & 0 & 0 & -\frac{J}{D} & 0 & 0 \\ 0 & 0 & \frac{J}{D} & J+w & 0 & 0 & 0 & 0 \\ 0 & \frac{2J}{D} & 0 & 0 & 2J+w & 0 & 0 & \frac{2J}{D} \\ 0 & 0 & -\frac{2J}{D} & 0 & 0 & w & 0 & 0 \\ 0 & 0 & 0 & \frac{4J}{D} & 0 & 0 & 2J+w & 0 \\ 0 & 0 & 0 & 0 & 0 & \frac{J}{D} & 0 & J+w \end{pmatrix}. \tag{3.23}$$

We can use the same method as in the reference [9] to solve \mathcal{U}_2 :

$$\mathcal{U}_2(t) \equiv \sum_{i=1}^8 f_a(t) e^{-iEt} F_a. \tag{3.24}$$

where $f_a(t)$ are given by

$$\begin{bmatrix} f_1(t) \\ f_2(t) \\ f_3(t) \\ f_4(t) \\ f_5(t) \\ f_6(t) \\ f_7(t) \\ f_8(t) \end{bmatrix} = \begin{bmatrix} 0 & 0 & \frac{1}{4} & \frac{1}{2} & \frac{1}{4} \\ 0 & \frac{D^2-2}{D(D^2-4)} & \frac{-1}{4(D-2)} & \frac{-1}{2D} & \frac{-1}{4(D+2)} \\ 0 & 0 & -\frac{1}{4} & 0 & \frac{1}{4} \\ 0 & \frac{-1}{D^2-4} & \frac{1}{4(D-2)} & 0 & \frac{-1}{4(D+2)} \\ \frac{1}{D^2-1} & \frac{-2}{D^2-4} & \frac{1}{2(D-1)(D-2)} & 0 & \frac{1}{2(D+1)(D+2)} \\ 0 & 0 & \frac{1}{4} & -\frac{1}{2} & \frac{1}{4} \\ \frac{-1}{D^3-D} & \frac{4}{D(D^2-4)} & \frac{-1}{2(D-1)(D-2)} & 0 & \frac{1}{2(D+1)(D+2)} \\ 0 & \frac{2}{D(D^2-4)} & \frac{-1}{4(D-2)} & \frac{1}{2D} & \frac{-1}{4(D+2)} \end{bmatrix} \times \begin{bmatrix} 1 \\ e^{-Jt} \\ e^{-(2-2D)^{-1}Jt} \\ e^{-2Jt} \\ e^{-(2+2D)^{-1}Jt} \end{bmatrix}. \quad (3.25)$$

Generally, we can calculate OTOC by using the expression of (3.24)

$$\text{Tr}(O_1(t)O_2O_3(t)O_4) = \begin{array}{c} O_1^T \\ O_3^T \\ \hline \text{ } \\ \hline O_2 \\ O_4 \end{array} \equiv \sum_{a=1}^8 f_a(t) \times \left(e^{-iEt} \mathbf{F}_a \right)_{O_1, O_2, O_3, O_4}. \quad (3.26)$$

A special case would be the noise-free case, which means that the noise strength J vanishes. We expect that the time evolution will be simplified into a unitary one. Note that from (3.25) we can directly find that all $f_a(t)$ vanishes except $f_1(t) = 1$. Hence

$$\text{Tr}(O_1(t)O_2O_3(t)O_4) = \left(e^{-iEt} \mathbf{F}_0 \right)_{O_1, O_2, O_3, O_4}. \quad (3.27)$$

which is just the unitary time evolution for a closed system and finishes our consistency check. Thus, we will be more confident to use (3.26) to calculate the fluctuations of two-point functions, spectral form factor (SFF) and other observables.

To end this section, we would mention that there is an alternative method [43] to evaluate $\mathcal{U}_2(t)$ by observing that

$$[\mathcal{L}_n, V^{\otimes n} \otimes V^{*\otimes n}] = 0, \quad \forall V \in U(D). \quad (3.28)$$

We can always decompose a wavefunction $\psi = \psi_{i_1 i_2}^{j_1 j_2} |i_1, j_1, i_2, j_2\rangle_{1\bar{1}2\bar{2}}$ into two singlets $\mathbf{1}$, four adjoints $\mathbf{D}^2 - \mathbf{1}$, an antisymmetric traceless \mathbf{A} , two mixed \mathbf{M} and a symmetric traceless \mathbf{S} rank $(2, 2)$ irreducible representations of $SU(D)$, with all the coefficients. Thus, we can also do the exponentiation on this basis. However, notice that the dimension of the representation is 10, which is larger than the number of independent graph categories 8, indicating that there are still some redundancies in the Young tableaux method. This might cause a longer processing time in numerical calculations.

4 Time Evolution for $n = 3$

Then we consider $n = 3$, so we have six sites: $\{1, \bar{1}, 2, \bar{2}, 3, \bar{3}\}$. The permutation group is $S_3 \otimes S_3$, $S_3 = \{I, X_{12}, X_{13}, X_{23}, X_{123}, X_{132}\}$, then

$$\mathcal{C} = \{(i, \bar{j})\}_{i, \bar{j}=1, 2, 3}, \quad \mathcal{E} = \{(i, j)\}_{1 \leq i < j \leq 3}, \quad \bar{\mathcal{E}} = \{(\bar{i}, \bar{j})\}_{1 \leq \bar{i} < \bar{j} \leq 3}. \quad (4.1)$$

Thus, $|\mathcal{C}| + |\mathcal{E}| + |\bar{\mathcal{E}}| = 15$, which is much more complicated than $n = 2$ case. However, we may get some hints from (2.12) that it is convenient to first classify the graphs by the number of paired vertices p , then to operate \mathcal{L}_3 on the graphs iteratively until we obtain all graph categories. The result shows that 720 individual graphs can be grouped into 26 categories. We present the basis in Table 3, labeling them by the permutations. Detailed discussions of the categories are provided in Sec. 4.1.

$\#F \backslash F_a$ p	I	$X + \bar{X}$	$X\bar{X}$	$XX + \bar{X}\bar{X}$	$XX\bar{X} + \bar{X}\bar{X}X$	$XX\bar{X}\bar{X}$
0	1	6	9	4	12	4
1	9	$18^{(e)}, 36^{(i)}$	$9^{(ee)}, 36^{(ei)}, 36^{(ii)}$	36	$36^{(e)}, 72^{(i)}$	36
2	18	$72^{(ei)}, 18^{(ii)}$	$36^{(ei,ei)}, 36^{(ei,ie)}, 72^{(ei,ii)}$	0	72	0
3	6	18	0	12	0	0

Table 3. The graph categories for $n = 3$.

4.1 Grouping Graphs into Categories

Here we first define some notations:

$$X \equiv \{X_{12}, X_{13}, X_{23}\}, [XX] \equiv \{X_{123}, X_{132}\}. \quad (4.2)$$

As discussed earlier, the number of individual graphs with p connected pairs is given by $N_{n,p} = (n!C_n^p)^2$. For $n = 3$, it is

$$N_{3,p} = \{36, 324, 324, 36\}, \quad \text{for } p = \{0, 1, 2, 3\}. \quad (4.3)$$

Next, we discuss the graph categories $F_{p,\alpha}$ with p connected pairs. For a graph with p pairs, notice that the second term in (2.16) ($\sum_{u \cap C[F]=\emptyset} c_u F$) represents graphs with $p+1$ pairs, while the last two terms indicate applying additional 2 swaps on F , which are excluded by $C(F)$.

- For $p = 0$, there are no restrictions on X .
- For $p = 1$, with $C[F] = c_u$, we should require $X \cap u = \emptyset$. We can define the allowed set $X^{(0)} = X^{(ex)}[u] \equiv \{X | X \cap u \neq \emptyset\}$ and its complement as $X^{(1)}$. For example, if $u = (1\bar{1})$, then we have $X^{(0)} = \{X_{23}\}$ and $X^{(1)} = X - X^{(0)} = \{X_{12}, X_{13}\}$.
- For $p > 1$, the condition $X \cap u = \emptyset$ cannot be satisfied when $n = 3$.

While the discussion of graph categories by connected pairs is complete for $n = 3$, we could generalize the definitions of $X^{(0)}$ and $X^{(1)}$ to $X^{(\alpha)}$ for generic n and p . We define the conditions set as follows

$$\text{Cons} \equiv \otimes^p \{ex, in\}. \quad (4.4)$$

For simplicity, we just denote $ex = 0, in = 1$, and define

$$\text{Con}(0, A, u) \equiv (A \cap u = \emptyset), \quad \text{Con}(1, A, u) \equiv (A \cap u \neq \emptyset), \quad (4.5)$$

showing that whether u intersects with A or not. Hence for a series of certain connected pairs u_1, u_2, \dots, u_p , $X^{(\alpha)}$ is a set of 2-swap operators:

$$X^{(\alpha)} = \{X_e | \cap_{j=1}^p \text{Con}(\alpha[j], e, u_j)\}. \quad (4.6)$$

In our case, for instance, we take $n = 3, p = 2$, then the condition set is $\text{Cons} = \{00, 01, 10, 11\}$. And if we further choose $u_1 = (1\bar{1}), u_2 = (2\bar{2})$, we have

$$X^{(00)} = \emptyset, X^{(01)} = \{X_{23}\}, X^{(10)} = \{X_{13}\}, X^{(11)} = \{X_{12}\}. \quad (4.7)$$

Equipped with the new categories $F_{0,I}$, we could calculate the operations of \mathcal{L}_n^r on those categories. We will find that $\mathcal{L}_n^r F_{0,I}$ can be expressed as a linear combination of graphs represented by permutations

$$\sum_{u_1, u_2, \dots, u_p} c(u_1, u_2, \dots, u_p) c \left[\prod_{j=1}^m (X + \bar{X})^{(\alpha_j)} \right] \quad (4.8)$$

where the product should be understood as the product between sets, which means the repeated terms should be eliminated. And the summation runs over all possible permutations. We will primarily discuss how to assign these blocks (4.8) into the appropriate graph categories in the followings.

Zero Pair: $C[F] = 0, \#F = 36$ For $p = 0$, (4.8) becomes

$$c \left[\prod_{j=1}^m (X + \bar{X}) \right], m = 0, 1, 2, 3, \dots. \quad (4.9)$$

Notice that for $n = 3$, we have the following relation for permutation sets

$$XX = 3I + 3[XX], [XX]X = 2X. \quad (4.10)$$

Hence all terms appearing in $(X + \bar{X})^m$ are

$$I, X + \bar{X}, X\bar{X}, [XX] + [\bar{X}\bar{X}], [XX]\bar{X} + [\bar{X}\bar{X}]X, [XX][\bar{X}\bar{X}]. \quad (4.11)$$

Since the gauge group vanishes, there is no redundancy. Hence we obtain 6 categories

$$F_{0,I}, F_{0,X+\bar{X}}, F_{0,X\bar{X}}, F_{0,[XX]+[\bar{X}\bar{X}]}, F_{0,[XX]\bar{X}+[\bar{X}\bar{X}]X}, F_{0,[XX][\bar{X}\bar{X}]}, \quad (4.12)$$

where $F_{0,A} \equiv c[A] = \cup_{x \in AC} c[x]$, or explicitly:

$$\begin{aligned}
F_{0,I} &\equiv c[I], \quad F_{0,X+\bar{X}} \equiv \sum_e c[X_e] + \sum_{\bar{e}} c[X_{\bar{e}}] + (X \leftrightarrow \bar{X}), \\
F_{0,X\bar{X}} &\equiv \sum_{u,\bar{e}} c[X_{\bar{e}}X_u] + (X \leftrightarrow \bar{X}), \\
F_{0,[XX]+[\bar{X}\bar{X}]} &\equiv c[X_{123}] + c[X_{132}] + c[X_{\bar{1}\bar{2}\bar{3}}] + c[X_{\bar{1}\bar{3}\bar{2}}] + (X \leftrightarrow \bar{X}), \\
F_{0,[XX]\bar{X}+[\bar{X}\bar{X}]X} &\equiv \sum_e c[X_{\bar{1}\bar{2}\bar{3}}X_e + X_{\bar{1}\bar{3}\bar{2}}X_e] + \sum_{\bar{e}} c[X_{123}X_{\bar{e}} + X_{132}X_{\bar{e}}] + (X \leftrightarrow \bar{X}), \\
F_{0,[XX][\bar{X}\bar{X}]} &\equiv c[X_{123}X_{\bar{1}\bar{2}\bar{3}}] + c[X_{123}X_{\bar{1}\bar{3}\bar{2}}] + c[X_{132}X_{\bar{1}\bar{2}\bar{3}}] + c[X_{132}X_{\bar{1}\bar{3}\bar{2}}] + (X \leftrightarrow \bar{X}).
\end{aligned} \tag{4.13}$$

It is straightforward to count their sizes, which are $\{1, 6, 9, 4, 12, 4\}$ respectively. Thus, we have $1 + 6 + 9 + 4 + 12 + 4 = 36$ graphs, as we have calculated in (4.3).

One Pair: $C[F] = 1, \#F = 324$ For $p = 1$, (4.8) becomes

$$\sum_u c_u \left[\prod_{j=1}^m (X + \bar{X})^{(\alpha_j)} \right], m = 0, 1, 2, 3, \dots, \alpha_j \in \{(0), (1)\}. \tag{4.14}$$

The size of the gauge group is just $p! = 1$, so there is no redundancy. For arbitrary $u = (i\bar{j})$, we find that

$$\#X^{(0)} = 1, \#X^{(1)} = 2, X = X^{(0)} + X^{(1)}. \tag{4.15}$$

Hence we have

$$X^{(0)}X^{(0)} = \{I\}, X^{(0)}X^{(1)} = X^{(1)}X^{(0)} = [XX], X^{(1)}X^{(1)} = 2I + 2[XX]. \tag{4.16}$$

All terms which can appear are

$$\begin{aligned}
&I, X^{(0)} + \bar{X}^{(0)}, X^{(1)} + \bar{X}^{(1)}, X^{(0)}\bar{X}^{(0)}, X^{(0)}\bar{X}^{(1)} + \bar{X}^{(0)}X^{(1)}, X^{(1)}\bar{X}^{(1)}, \\
&[XX] + [\bar{X}\bar{X}], [XX]\bar{X}^{(0)} + [\bar{X}\bar{X}]X^{(0)}, [XX]\bar{X}^{(1)} + [\bar{X}\bar{X}]X^{(1)}, [XX][\bar{X}\bar{X}].
\end{aligned} \tag{4.17}$$

So there are 10 categories

$$F_{1,I}, F_{1,X}^{(0)}, F_{1,X}^{(1)}, F_{1,X\bar{X}}^{(00)}, F_{1,X\bar{X}}^{(01)}, F_{1,X\bar{X}}^{(11)}, F_{1,XX}, F_{1,XX\bar{X}}^{(0)}, F_{1,XX\bar{X}}^{(1)}, F_{1,XX\bar{X}\bar{X}} \tag{4.18}$$

with there sizes to be $\{1, 18, 36, 9, 36, 36, 36, 72, 36\}$.

Two Pairs: $C[F] = 2, \#F = 324$ For $p = 2$, (4.8) becomes

$$\sum_{u,v} c_u c_v \left[\prod_{j=1}^m (X + \bar{X})^{(\alpha_j)} \right], m = 0, 1, 2, 3, \dots, \alpha_j \in \{(00), (01), (10), (11)\}. \tag{4.19}$$

$\forall u, v, u \cap v = \emptyset$, we have

$$X^{(00)} = \emptyset, X = \{X^{(01)}, X^{(10)}, X^{(11)}\}. \quad (4.20)$$

So all terms which can appear are

$$\begin{aligned} & I, X^{(01)+(10)} + \bar{X}^{(01)+(10)}, X^{(11)} + \bar{X}^{(11)}, X^{(01)}\bar{X}^{(01)} + X^{(10)}\bar{X}^{(10)}, \\ & X^{(01)}\bar{X}^{(10)} + X^{(10)}\bar{X}^{(01)}, X^{(01)+(10)}\bar{X}^{(11)} + X^{(11)}\bar{X}^{(01)+(10)}, X^{(11)}\bar{X}^{(11)}, [XX] + [\bar{X}\bar{X}], \\ & [XX]\bar{X}^{(01)+(10)} + [\bar{X}\bar{X}]X^{(01)+(10)}, [XX]\bar{X}^{(11)} + [\bar{X}\bar{X}]X^{(11)}, [XX][\bar{X}\bar{X}]. \end{aligned} \quad (4.21)$$

But for $p = 2$, the gauge group generated by $X^{(11)} \otimes \bar{X}^{(11)}$ has size $p! = 2$. We have the equivalent relation

$$c_u c_v c[\sigma] = c_u c_v c\left[\sigma \cdot X^{(11)}\bar{X}^{(11)}\right], \quad (4.22)$$

which means $X^{(11)}\bar{X}^{(11)} \sim I$, and furthermore

$$\begin{aligned} [XX] &\sim [XX]X^{(11)}\bar{X}^{(11)} = X^{(10)+(01)}\bar{X}^{(11)}, \\ [XX][\bar{X}\bar{X}] &\sim [XX]X^{(11)}[\bar{X}\bar{X}]\bar{X}^{(11)} = X^{(10)+(01)}\bar{X}^{(10)+(01)}, \\ [XX]\bar{X}^{(11)} &\sim [XX]X^{(11)}\bar{X}^{(11)}\bar{X}^{(11)} = X^{(10)+(01)}. \end{aligned} \quad (4.23)$$

So we only have 7 categories

$$F_{2,I}, F_{2,X}^{(01)}, F_{2,X}^{(11)}, F_{2,X\bar{X}}^{(01,01)}, F_{2,X\bar{X}}^{(01,10)}, F_{2,X\bar{X}}^{(01,11)}, F_{2,XX\bar{X}}. \quad (4.24)$$

Their sizes are $\{18, 72, 18, 36, 36, 72, 72\}$.

Three Pairs: $C[F] = 3, \#F = 36$ For $p = 2$, (4.8) becomes

$$\sum_{u_1, u_2, u_3} c_{u_1} c_{u_2} c_{u_3} \left[\prod_{j=1}^m (X + \bar{X})^{(\alpha_j)} \right], m = 0, 1, 2, 3, \dots \quad (4.25)$$

For three pairs u_1, u_2, u_3 , we can only take three conditions

$$\alpha_j \in \{(011), (101), (110)\}. \quad (4.26)$$

Any permutation $X_e X_{\bar{e}}$ is considered as a redundancy, allowing us to fix the order of $\bar{1}, \bar{2}, \bar{3}$. This means we only need to consider permutations of $1, 2, 3$. Utilizing the fact that $X = X^{(011)} + X^{(101)} + X^{(110)}$, we identify three building blocks: $I, X, [XX]$. The respective graph categories are:

$$F_{3,I} = \cup_{u_1, u_2, u_3} c[I], F_{3,X} = \cup_u c_{u_1} c_{u_2} c_{u_3} c[X], F_{3,XX} = \cup_{u_1, u_2, u_3} c_{u_1} c_{u_2} c_{u_3} c[[XX]]. \quad (4.27)$$

They have sizes of $\{6, 18, 12\}$, respectively.

4.2 Operation of \mathcal{L}_3

Using the relations for $n = 3$

$$\begin{aligned} XX &= 3I + 3[XX], [XX]X = 2X, \\ XX_e &= X_e + [XX], [XX]X_e = X_e[XX] = X - X_e, \end{aligned} \quad (4.28)$$

and the gauge symmetry discussed earlier, it is straightforward to calculate the operation of \mathcal{L}_3 on the graph categories defined in the previous section. For simplicity, we define \mathcal{L}'_n as the non-trivial part of \mathcal{L}_n :

$$\mathcal{L}_n \mathbf{F}_{p,\alpha} = (w + pJ) \mathbf{F}_{p,\alpha} + \mathcal{L}'_n \mathbf{F}_{p,\alpha}. \quad (4.29)$$

With some calculations one can get:

Zero Pair: $\mathbf{F}_{0,I}, \mathbf{F}_{0,X}, \mathbf{F}_{0,X\bar{X}}, \mathbf{F}_{0,XX}, \mathbf{F}_{0,XX\bar{X}}, \mathbf{F}_{0,XX\bar{X}\bar{X}}$

$$\begin{aligned} \mathcal{L}'_3 \mathbf{F}_{0,I} &= \frac{J}{D} \mathbf{F}_{1,I} - \frac{J}{D} \mathbf{F}_{0,X}, \\ \mathcal{L}'_3 \mathbf{F}_{0,X} &= \frac{J}{D} \left(\mathbf{F}_{1,X}^{(0)} + \mathbf{F}_{1,X}^{(1)} \right) - \frac{J}{D} \left(6\mathbf{F}_{0,I} + 3\mathbf{F}_{0,XX} + 2\mathbf{F}_{0,X\bar{X}} \right), \\ \mathcal{L}'_3 \mathbf{F}_{0,X\bar{X}} &= \frac{J}{D} \left(\mathbf{F}_{1,X\bar{X}}^{(00)} + \mathbf{F}_{1,X\bar{X}}^{(11)} + \mathbf{F}_{1,X\bar{X}}^{(01)} \right) - \frac{J}{D} \left(3\mathbf{F}_{0,X} + 3\mathbf{F}_{0,XX\bar{X}} \right), \\ \mathcal{L}'_3 \mathbf{F}_{0,XX} &= \frac{J}{D} \mathbf{F}_{1,XX} - \frac{J}{D} \left(2\mathbf{F}_{0,X} + \mathbf{F}_{0,XX\bar{X}} \right), \\ \mathcal{L}'_3 \mathbf{F}_{0,XX\bar{X}} &= \frac{J}{D} \left(\mathbf{F}_{1,XX\bar{X}}^{(0)} + \mathbf{F}_{1,XX\bar{X}}^{(1)} \right) - \frac{J}{D} \left(4\mathbf{F}_{0,X\bar{X}} + 3\mathbf{F}_{0,XX} + 6\mathbf{F}_{0,XX\bar{X}\bar{X}} \right), \\ \mathcal{L}'_3 \mathbf{F}_{0,XX\bar{X}\bar{X}} &= \frac{J}{D} \mathbf{F}_{1,XX\bar{X}\bar{X}} - \frac{2J}{D} \mathbf{F}_{0,XX\bar{X}}. \end{aligned} \quad (4.30)$$

One Pair: $\mathbf{F}_{1,I}, \mathbf{F}_{1,X}^{(0)}, \mathbf{F}_{1,X}^{(1)}, \mathbf{F}_{1,X\bar{X}}^{(00)}, \mathbf{F}_{1,X\bar{X}}^{(01)}, \mathbf{F}_{1,X\bar{X}}^{(11)}, \mathbf{F}_{1,XX}, \mathbf{F}_{1,XX\bar{X}}^{(0)}, \mathbf{F}_{1,XX\bar{X}}^{(1)}, \mathbf{F}_{1,XX\bar{X}\bar{X}}$

$$\begin{aligned} \mathcal{L}'_3 \mathbf{F}_{1,I} &= \frac{2J}{D} \mathbf{F}_{2,I} - \frac{J}{D} \mathbf{F}_{1,X}^{(0)}, \\ \mathcal{L}'_3 \mathbf{F}_{1,X}^{(0)} &= \frac{J}{D} \mathbf{F}_{2,X}^{(01)} - \frac{J}{D} \left(2\mathbf{F}_{1,I} + 2\mathbf{F}_{1,X\bar{X}}^{(00)} \right), \\ \mathcal{L}'_3 \mathbf{F}_{1,X}^{(1)} &= \frac{J}{D} \left(\mathbf{F}_{2,X}^{(01)} + 4\mathbf{F}_{2,X}^{(11)} \right) - \frac{J}{D} \left(\mathbf{F}_{1,XX} + \mathbf{F}_{1,X\bar{X}}^{(01)} \right), \\ \mathcal{L}'_3 \mathbf{F}_{1,XX} &= \frac{2J}{D} \mathbf{F}_{2,XX}^{(01,11)} - \frac{J}{D} \left(\mathbf{F}_{1,X}^{(1)} + \mathbf{F}_{1,XX\bar{X}}^{(0)} \right), \\ \mathcal{L}'_3 \mathbf{F}_{1,X\bar{X}}^{(00)} &= \frac{J}{D} \mathbf{F}_{2,X\bar{X}}^{(01,01)} - \frac{J}{D} \mathbf{F}_{1,X}^{(0)}, \\ \mathcal{L}'_3 \mathbf{F}_{1,X\bar{X}}^{(01)} &= \frac{J}{D} \left(2\mathbf{F}_{2,X\bar{X}}^{(01,10)} + \mathbf{F}_{2,X\bar{X}}^{(01,11)} \right) - \frac{J}{D} \left(\mathbf{F}_{1,X}^{(1)} + \mathbf{F}_{1,XX\bar{X}}^{(0)} \right), \\ \mathcal{L}'_3 \mathbf{F}_{1,X\bar{X}}^{(11)} &= \frac{J}{D} \left(\mathbf{F}_{2,X\bar{X}}^{(01,01)} + \mathbf{F}_{2,X\bar{X}}^{(01,11)} + 2\mathbf{F}_{2,I} \right) - \frac{J}{D} \mathbf{F}_{1,XX\bar{X}}^{(1)}, \\ \mathcal{L}'_3 \mathbf{F}_{1,XX\bar{X}}^{(0)} &= \frac{2J}{D} \mathbf{F}_{2,XX\bar{X}} - \frac{J}{D} \left(\mathbf{F}_{1,XX} + \mathbf{F}_{1,X\bar{X}}^{(01)} \right), \end{aligned}$$

It is straightforward to obtain the spectrum of M_J :

$$\left\{ 0, 0, 0, -\frac{3(D-2)J}{D}, -\frac{3(D-1)J}{D}, -\frac{2(D-1)J}{D}, -\frac{2(D-1)J}{D}, -\frac{2(D-1)J}{D}, \right. \\ \left. -3J, -3J, -2J, -2J, -2J, -2J, -J, -J, -J, -J, -J, -J, -J, \right. \\ \left. -\frac{3(D+1)J}{D}, -\frac{2(D+1)J}{D}, -\frac{2(D+1)J}{D}, -\frac{2(D+1)J}{D}, -\frac{3(D+2)J}{D} \right\}. \quad (4.34)$$

Then we can find the analytical expression of $\mathcal{U}_3(t)$ as

$$\mathcal{U}_3(t) = e^{\mathcal{L}_3 t} = e^{-iEt} \sum_{a=1}^{26} f_a(t) \mathbf{F}_a. \quad (4.35)$$

We plot $f_a(t)$ in Fig.3, while the explicit expressions are given in Appendix A. Generally, we

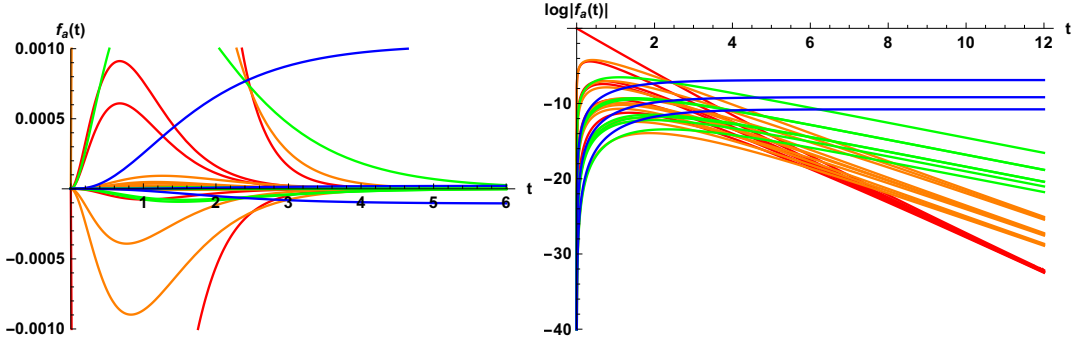


Figure 3. The pattern coefficient $f_a(t)$ and its log-plot, where we set $D = 10$ and $J = 1$. We depict the categories of $p = 0, 1, 2, 3$ with red, orange, green, and blue colors, respectively. One can see that the three categories with $p = 3$ have energy 0, so they (the blue lines) remain finite at time $t = \infty$.

can calculate the correlation functions as

$$\text{Tr} [O_1(t)O_2O_3(t)O_4O_5(t)O_6] = \begin{array}{c} O_1^T \\ O_3^T \\ O_5^T \end{array} \begin{array}{c} \boxed{u_3} \\ \end{array} \begin{array}{c} O_2^T \\ O_4^T \\ O_6 \end{array} \equiv \sum_{a=1}^{26} f_a(t) \times \left(e^{-iEt} \mathbf{F}_a \right)_{O_1, O_2, O_3, O_4, O_5, O_6} \quad (4.36)$$

where we have used $O(t) \equiv U^\dagger O U$ and the graph representation for an operator A

$$A_{ij} = \begin{array}{c} | \\ \boxed{A} \\ | \end{array} \begin{array}{c} i \\ j \end{array}. \quad (4.37)$$

To calculate $F_a[O_1, O_2, O_3, O_4, O_5, O_6]$, in principle, we need to contract each individual graph in the category with the operator tensor in the way as shown in (4.36). The expression $F = \prod_{i=1}^p c_{a_i \bar{b}_i} c[\sigma]$ has told us the connection between points in the graph. We treat the connections in the graph as free propagators and the operators as bridges between points i, \bar{i} and $\bar{i}', (\bar{i} + 1)'$, where the prime means that the point is on the right-hand side of the graph. So there is no need to draw the graph. We can just start with any points following the connections in the graph and form a closed loop. Hence we will have a trace of operators

$$\text{Tr}(O_i O_j O_k^T \cdots) . \quad (4.38)$$

If there are still points that we have not passed, we then start with those points, finding another closed loop until all points in the graph have been visited. The process may be a bit tedious, but it can be accomplished with some code. Alternatively, one can simply write down the explicit expression of a graph using the Kronecker delta function as defined in (2.9).

Moreover, with the expression of $\mathcal{U}_{1,2,3}(t)$, one can calculate the correlation function with general time order $\text{Tr}[O_1(t_1)O_2O_3(t_2)O_4O_5(t_3)O_6]$. For example, we consider the case $t_1 < t_2 < t_3$, then the ensemble-averaged time-evolution $\mathcal{U}_3(t_1, t_2, t_3)$ is

$$\begin{aligned} & \mathbb{E}(\mathbb{I}_D^{\otimes 2} \otimes \mathbb{I}_D^{\otimes 2} \otimes U(t_{32}) \otimes U^*(t_{32})) \mathbb{E}(\mathbb{I}_D \otimes \mathbb{I}_D \otimes U(t_{21})^{\otimes 2} \otimes U^*(t_{21})^{\otimes 2}) \mathbb{E}(U(t_1)^{\otimes 3} \otimes U^*(t_1)^{\otimes 3}) \\ &= [\mathbb{I}_D^{\otimes 2} \otimes \mathbb{I}_D^{\otimes 2} \otimes \mathcal{U}_1(t_{32})] \times [\mathbb{I}_D \otimes \mathbb{I}_D \otimes \mathcal{U}_2(t_{21})] \times \mathcal{U}_3(t_1) , \end{aligned} \quad (4.39)$$

where \mathbb{I}_D denotes the D -dimensional identity matrix. Finally, we simply need to contract $\mathcal{U}_3(t_1, t_2, t_3)$ with the operator tensor as demonstrated in (4.36). In this paper, we do not provide explicit expressions for the correlation functions.

5 General Cases

For general n , we have $2n$ sites $\{1, \bar{1}, 2, \bar{2}, 3, \bar{3}, \dots, n, \bar{n}\}$. The permutation group is $S_n \otimes S_n$. As discussed in $n = 3$ case, we should define

$$X^{(\alpha_j)} \equiv \{X_e | \cap_{k=1}^p \text{Con}(\alpha_j[k], e, u_k)\} . \quad (5.1)$$

$X^{(\alpha_j)}$ is a set of 2-swap operators submitting to the condition α_j . Our primary goal is to deal with the following graph expression

$$\sum_{u_1, u_2, \dots, u_p} c(u_1, u_2, \dots, u_p) c \left[\prod_{j=1}^m (X + \bar{X})^{(\alpha_j)} \right] , \quad (5.2)$$

and assign them into appropriate categories.

Since it is free to change the order of u_1, u_2, \dots, u_p , there is a S_p permutation redundancy for the conditions:

$$\{\alpha_j\}_{j=1,2,\dots,p} \sim \{\sigma \alpha_j\}_{j=1,2,\dots,p}, \quad \forall \sigma \in S_p . \quad (5.3)$$

In practice, we can always find a permutation $\sigma \in S_n$ as a product of cycles $\{\sigma_i\}_{i=1,2,\dots,g}$ with length $1 < l_1 \leq l_2 \dots \leq l_g$ such that:

$$X_{[l_1, l_2, \dots, l_g]} \equiv \{X_{\sigma_1 \sigma_2 \dots \sigma_g} \mid |\sigma_i| = l_i, \sigma_i \cap \sigma_j = \emptyset, i \neq j\} . \quad (5.4)$$

Then for a certain p , we first analyze all permutation categories appearing in the products $\prod_{j=1}^m X^{(\alpha_j)}$, $m = 0, 1, 2, \dots$, which gives us a division of the permutation group S_n

$$S_n = \cup_{\alpha=1}^{N_X} X_\alpha, X_\alpha \cap X_\beta = \emptyset, \forall \alpha \neq \beta . \quad (5.5)$$

So naively we have $\frac{N_X(N_X+1)}{2}$ graph categories:

$$F_{p, X_\alpha \bar{X}_\beta} \equiv \cup_{x \in X_\alpha \bar{X}_\beta \cup X_\beta \bar{X}_\alpha} \cup_{u_1, u_2, \dots, u_p} c(u_1, u_2, \dots, u_p) c[x] . \quad (5.6)$$

Finally when $p \geq 2$, we need to consider removing the permutation redundancy of the conditions and the gauge symmetry of the graph representation. In other words, we need to module some equivalent relations.

5.1 Example: $n = 4$

Here we take $n = 4$ as an example. For different number of connected pairs, the number of graphs should be $N_{4,p} = \{576, 9216, 20736, 9216, 576\}$. We then define

$$X_{[2]} \equiv X = \{X_{12}, X_{13}, X_{14}, X_{23}, X_{24}, X_{34}\} . \quad (5.7)$$

Like what we do for $n = 3$ case, we discuss the graph categories according to the number of pairs.

Zero Pair $p = 0, \#F = 576$ For $p = 0$, there is no restriction on X , so we have the division of S_4 as

$$S_4 = I + X_{[2]} + X_{[3]} + X_{[2,2]} + X_{[4]}, \#S_4 = 1 + 6 + 8 + 3 + 6 = 24 . \quad (5.8)$$

Since there is no permutation redundancy or gauge redundancy, we have $\frac{N_X(N_X+1)}{2} = 15$ independent graph categories:

$$\begin{aligned} & F_{0,I}, F_{0,X}, F_{0,X_{[3]}}, F_{0,X_{[2,2]}}, F_{0,X_{[4]}}, F_{0,X\bar{X}}, F_{0,X\bar{X}_{[3]}}, F_{0,X\bar{X}_{[2,2]}}, F_{0,X\bar{X}_{[4]}}, F_{0,X_{[3]}\bar{X}_{[3]}}, \\ & F_{0,X_{[3]}\bar{X}_{[2,2]}}, F_{0,X_{[3]}\bar{X}_{[4]}}, F_{0,X_{[2,2]}\bar{X}_{[2,2]}}, F_{0,X_{[2,2]}\bar{X}_{[4]}}, F_{0,X_{[4]}\bar{X}_{[4]}} . \end{aligned} \quad (5.9)$$

One Pair $p = 1, \#F = 9216$ For an arbitrary pair u , we have two conditions for X and $X_{[3]}$, so that we have the division

$$S_4 = I + X^{(0)} + X^{(1)} + X_{[3]}^{(0)} + X_{[3]}^{(1)} + X_{[2,2]} + X_{[4]} \equiv \cup_{\alpha=1}^7 X_\alpha . \quad (5.10)$$

Since $p < 2$, there is no permutation or gauge redundancy, so we have $\frac{7 \times 8}{2} = 28$ categories:

$$F_{1, X_\alpha \bar{X}_\beta} \equiv \sum_u \sum_{x \in X_\alpha \bar{X}_\beta \cup X_\beta \bar{X}_\alpha} c_u c[x] . \quad (5.11)$$

Two Pairs $p = 2, \#F = 20736$ For any two pairs u_1, u_2 , we find

$$X = X^{(00)} + X^{(01)} + X^{(10)} + X^{(11)}, \quad X_{[3]}^{(00)} = \emptyset, \quad X_{[3]} = X_{[3]}^{(01)} + X_{[3]}^{(10)} + X_{[3]}^{(11)}, \quad (5.12)$$

so we obtain the division to be

$$S_4 = I + X^{(00)} + X^{(01)} + X^{(10)} + X^{(11)} + X_{[3]}^{(01)} + X_{[3]}^{(10)} + X_{[3]}^{(11)} + X_{[2,2]} + X_{[4]}. \quad (5.13)$$

Naively, we have $\frac{10 \times 11}{2} = 55$ categories. But here we need to remove the permutation redundancy. For an example, changing the order of conditions α_j , we have

$$F_{2,X}^{(01)} = F_{2,X}^{(10)}, \quad F_{2,X\bar{X}}^{(00,01)} = F_{2,X\bar{X}}^{(00,10)}. \quad (5.14)$$

And notice the symmetry between X and \bar{X} , we have

$$F_{2,X\bar{X}}^{(00,01)} = F_{2,X\bar{X}}^{(01,00)}. \quad (5.15)$$

As for the gauge redundancy, here we impose the equivalence $X^{(11)}\bar{X}^{(11)} \sim I$, so immediately we have

$$F_{2,X\bar{X}}^{(11,11)} = F_{2,I}. \quad (5.16)$$

There are other equivalence between categories, we will not shown them here. After removing all redundancy, we will obtain the proper graph categories for $p = 2$.

Three pairs For three pairs, we have

$$\begin{aligned} X &= X^{(001)} + X^{(010)} + X^{(100)} + X^{(011)} + X^{(101)} + X^{(110)}, \\ X_{[3]} &= X_{[3]}^{(011)} + X_{[3]}^{(101)} + X_{[3]}^{(110)}, \end{aligned} \quad (5.17)$$

so we obtain the division as

$$\begin{aligned} S_4 &= I + X^{(001)} + X^{(010)} + X^{(100)} + X^{(011)} + X^{(101)} + X^{(110)} \\ &\quad + X_{[3]}^{(011)} + X_{[3]}^{(101)} + X_{[3]}^{(110)} + X_{[2,2]} + X_{[4]}. \end{aligned} \quad (5.18)$$

Naively, there are $\frac{12 \times 13}{2} = 96$ categories. The permutation redundancy is similar to $p = 2$ case and the gauge group is generated by

$$X^{(011)}\bar{X}^{(011)}, X^{(101)}\bar{X}^{(101)}, X^{(110)}\bar{X}^{(110)}. \quad (5.19)$$

After removing the all redundancy, the number of categories will be much smaller.

Four Pairs We notice that

$$\begin{aligned} X &= X^{(0011)} + X^{(0101)} + X^{(1001)} + X^{(0110)} + X^{(1010)} + X^{(1100)} , \\ X_{[3]} &= X_{[3]}^{(0111)} + X_{[3]}^{(1011)} + X_{[3]}^{(1101)} + X_{[3]}^{(1110)} , \end{aligned} \quad (5.20)$$

which gives the division as

$$\begin{aligned} S_4 &= I + X^{(0011)} + X^{(0101)} + X^{(1001)} + X^{(0110)} + X^{(1010)} + X^{(1100)} \\ &\quad + X_{[3]}^{(011)} + X_{[3]}^{(101)} + X_{[3]}^{(110)} + X_{[2,2]} + X_{[4]} . \end{aligned} \quad (5.21)$$

Notice the gauge group is generated by each permutation like $X_e \bar{X}_e$. So we can fix the order of \bar{i} to be $\bar{1}\bar{2}\bar{3}\bar{4}$, and we just need to consider the categories

$$\mathbf{F}_\alpha \equiv \cup_{u_1, u_2, u_3, u_4} c(u_1, u_2, u_3, u_4) c[X_\alpha] . \quad (5.22)$$

Notice the permutation redundancy, we have

$$X^{(0011)} \sim X^{(0101)} \sim X^{(1001)} \sim X^{(0110)} \sim X^{(1010)} \sim X^{(1100)}, X_{[3]}^{(011)} \sim X_{[3]}^{(101)} \sim X_{[3]}^{(110)} , \quad (5.23)$$

so we only have five categories left

$$\mathbf{F}_{4,I}, \mathbf{F}_{4,X}, \mathbf{F}_{4,X_{[3]}}, \mathbf{F}_{4,X_{[2,2]}}, \mathbf{F}_{4,X_{[4]}} . \quad (5.24)$$

6 Discussions and Outlook

In this paper we analyze the time evolution of the n -replica physics of the BGUE model in a graph-based framework. This approach proves to be particularly effective for lower values of n , as explicitly demonstrated in the $n = 2$ and $n = 3$ cases. We also provide a systematic strategy that extends to generic n . Our construction highlights how the increasing complexity of graph structures can be managed by organizing them into well-defined categories, which will simplify the calculations of two-point functions, OTOC, and other relevant observables.

The general formulation outlined in Sec. 5 suggests that this method can, in principle, be extended to arbitrary n . However, as n increases, the growing number of graph structures presents significant challenges. Addressing these challenges will require the development of more efficient techniques for classifying, encoding, and manipulating graphs at large n . An important direction for future research is to explore algorithmic approaches to systematically handle this complexity. Moreover, further investigation into the implications of this framework for Brownian disordered systems and quantum information theory may uncover deeper structural insights into the role of replica dynamics in random matrix models.

A key insight is that the factor w , which encodes the dependence on the system spectrum, commutes with the graph-based operators. This allows us to analyze the system with infinite-temperature GUE noise without introducing additional complexity.

It is worth noting that the techniques developed in this paper can also be applied to other models, such as the Brownian Gaussian Orthogonal Ensemble (BGOE) and the Brownian Gaussian Symplectic Ensemble (BGSE). In particular, for BGOE, we have:

$$\mathcal{L}_n = \frac{-JD}{D+1} \left[n\mathbb{I} + \sum_{i<j} (P_{ij} + P_{\bar{i}\bar{j}}) - \sum_{i,\bar{j}} P_{i\bar{j}} \right] + \frac{-J}{D+1} \left[n + \sum_{i<j} X_{ij} + X_{\bar{i}\bar{j}} - \sum_{i,\bar{j}} X_{i\bar{j}} \right], \quad (6.1)$$

and for BGSE:

$$\mathcal{L}_n = \frac{-J}{D-1} \left[2n(D-1)\mathbb{I} - D \sum_{i<j} (P_{ij} + P_{\bar{i}\bar{j}}) - 2D \sum_{i,\bar{j}} P_{i\bar{j}} + 4 \sum_{i<j} (X_{ij} + X_{\bar{i}\bar{j}}) + 2 \sum_{i,\bar{j}} X_{i\bar{j}} \right]. \quad (6.2)$$

We find there are new operators such as $P_{ij}, P_{\bar{i}\bar{j}}, X_{i\bar{j}}$. Hence an individual graph appearing in \mathcal{L}_n^r can be written as

$$\mathbb{F} = \prod_{i=1}^{p_1} c_{a_i a'_i} \prod_{i=1}^{p_2} c_{\bar{b}_i \bar{b}'_i} \prod_{i=1}^{p_3} c_{r_i \bar{s}_i} c[\sigma]. \quad (6.3)$$

As a result, when n increases, the introduction of new operators in BGOE and BGSE further complicates the graph structures, leading to a greater number of individual graphs that become increasingly challenging to systematically organize them into appropriate categories. While this classification seems to be complicated, it is, at its core, a well-structured problem. As discussed in the introduction, the method presented in this paper is fundamentally equivalent to the approach outlined in [43]. Moreover, the inherent symmetry of \mathcal{L}_n in the BGUE, BGOE, and BGSE cases simplifies its diagonalization, which is closely related to a well-studied mathematical problem: the decomposition of the direct product of fundamental representations. Given this, we expect that the techniques developed in this work can also be successfully extended to models without obvious symmetry, further demonstrating the power and versatility of the proposed framework.

Acknowledgment

The authors would like to thank Haifeng Tang, Yingyu Yang, and Yanyuan Li for their valuable discussions and comments during the preparation of this work. CP, JY and TL are supported by NSFC NO. 12175237, CP is also supported in part by NSFC NO. 12447108, NSFC NO. 12247103, the Fundamental Research Funds for the Central Universities, and funds from the Chinese Academy of Sciences.

A Expression of $\mathcal{U}_3(t)$

As discussed in Sec.4, we write $\mathcal{U}_3 = \sum_{a=1}^{26} f_a(t) e^{-iEt} \mathbf{F}_a$. Here we list the explicit expressions for f_a . For simplicity, we denote

$$f_a(t) = \mathbf{v}_a \cdot \boldsymbol{\xi}(t), \quad (\text{A.1})$$

where $\boldsymbol{\xi}(t)$ are 10 wavefunctions.

$$\boldsymbol{\xi}(t) = \left\{ e^{-Jt}, e^{-2Jt}, e^{-\frac{2(D+1)Jt}{D}}, e^{-\frac{2(D-1)Jt}{D}}, e^{-3Jt}, e^{-\frac{3(D+1)Jt}{D}}, e^{-\frac{3(D-1)Jt}{D}}, e^{-\frac{3(D+2)Jt}{D}}, e^{-\frac{3(D-2)Jt}{D}}, 1 \right\}, \quad (\text{A.2})$$

and the 26 vectors are

$$\begin{aligned} \mathbf{v}_1 &= \left\{ 0, 0, 0, 0, \frac{1}{2}, \frac{2}{9}, \frac{2}{9}, \frac{1}{36}, \frac{1}{36}, 0 \right\}, \\ \mathbf{v}_2 &= \left\{ 0, 0, 0, 0, 0, \frac{1}{9}, -\frac{1}{9}, \frac{1}{36}, -\frac{1}{36}, 0 \right\}, \\ \mathbf{v}_3 &= \left\{ 0, 0, 0, 0, -\frac{1}{18}, 0, 0, \frac{1}{36}, \frac{1}{36}, 0 \right\}, \\ \mathbf{v}_4 &= \left\{ 0, 0, 0, 0, -\frac{1}{6}, \frac{1}{18}, \frac{1}{18}, \frac{1}{36}, \frac{1}{36}, 0 \right\}, \\ \mathbf{v}_5 &= \left\{ 0, 0, 0, 0, 0, -\frac{1}{18}, \frac{1}{18}, \frac{1}{36}, -\frac{1}{36}, 0 \right\}, \\ \mathbf{v}_6 &= \left\{ 0, 0, 0, 0, \frac{1}{6}, -\frac{1}{9}, -\frac{1}{9}, \frac{1}{36}, \frac{1}{36}, 0 \right\}, \\ \mathbf{v}_7 &= \left\{ 0, \frac{5-D^2}{18D-2D^3}, \frac{D^2+3D-2}{4(D-2)(D+1)(D+4)}, \frac{D^2-3D-2}{4(D-4)(D-1)(D+2)}, \right. \\ &\quad \left. -\frac{20-9D^2}{72D-18D^3}, -\frac{2(D+2)}{9(D+1)(D+3)}, -\frac{2(D-2)}{9(D^2-4D+3)}, -\frac{1}{36(D+4)}, \frac{1}{144-36D}, 0 \right\}, \\ \mathbf{v}_8 &= \left\{ 0, 0, \frac{D^2+3D-2}{4(D-2)(D+1)(D+4)}, \frac{-D^2+3D+2}{4(D^3-3D^2-6D+8)}, \frac{4}{36-9D^2}, \right. \\ &\quad \left. -\frac{1}{9D+9}, \frac{1}{9(D-1)}, -\frac{1}{36(D+4)}, \frac{1}{36(D-4)}, 0 \right\}, \\ \mathbf{v}_9 &= \left\{ 0, \frac{1}{18-2D^2}, -\frac{D+2}{4(D^3+3D^2-6D-8)}, -\frac{D-2}{4(D-4)(D-1)(D+2)}, \right. \\ &\quad \left. \frac{2}{9(D^2-4)}, -\frac{2D+3}{18(D+1)(D+3)}, \frac{2D-3}{18(D-3)(D-1)}, -\frac{1}{36(D+4)}, \frac{1}{36(D-4)}, 0 \right\}, \\ \mathbf{v}_{10} &= \left\{ 0, -\frac{D^2-5}{2D(D^2-9)}, \frac{D^2+3D-2}{4(D-2)(D+1)(D+4)}, \frac{D^2-3D-2}{4(D-4)(D-1)(D+2)}, \frac{20-D^2}{72D-18D^3}, \right. \end{aligned}$$

$$\begin{aligned}
& \left. -\frac{2}{9(D+1)(D+3)}, \frac{2}{9(D^2-4D+3)}, -\frac{1}{36(D+4)}, \frac{1}{144-36D}, 0 \right\}, \\
\mathbf{v}_{11} = & \left\{ 0, \frac{1}{18D-2D^3}, -\frac{D+2}{4(D^3+3D^2-6D-8)}, \frac{D-2}{4(D-4)(D-1)(D+2)}, -\frac{D^2+4}{72D-18D^3}, \right. \\
& \left. -\frac{1}{18(D+1)(D+3)}, \frac{1}{18(D^2-4D+3)}, -\frac{1}{36(D+4)}, \frac{1}{144-36D}, 0 \right\}, \\
\mathbf{v}_{12} = & \left\{ 0, \frac{1}{D(D^2-9)}, \frac{1}{2(D-2)(D+1)(D+4)}, \frac{1}{2(D^3-3D^2-6D+8)}, \frac{8-D^2}{72D-18D^3}, \right. \\
& \left. \frac{1}{9(D^2+4D+3)}, -\frac{1}{9(D^2-4D+3)}, -\frac{1}{36(D+4)}, \frac{1}{144-36D}, 0 \right\}, \\
\mathbf{v}_{13} = & \left\{ 0, -\frac{1}{18D-2D^3}, -\frac{D+2}{4(D^3+3D^2-6D-8)}, \frac{D-2}{4(D-4)(D-1)(D+2)}, \frac{4-3D^2}{72D-18D^3}, \right. \\
& \left. -\frac{D+2}{18(D+1)(D+3)}, -\frac{D-2}{18(D^2-4D+3)}, -\frac{1}{36(D+4)}, \frac{1}{144-36D}, 0 \right\}, \\
\mathbf{v}_{14} = & \left\{ 0, \frac{1}{2(D^2-9)}, -\frac{D+2}{4(D^3+3D^2-6D-8)}, -\frac{D-2}{4(D-4)(D-1)(D+2)}, \frac{2}{9(D^2-4)}, \right. \\
& \left. \frac{D}{18(D^2+4D+3)}, -\frac{D}{18(D^2-4D+3)}, -\frac{1}{36(D+4)}, \frac{1}{36(D-4)}, 0 \right\}, \\
\mathbf{v}_{15} = & \left\{ 0, 0, \frac{1}{2(D-2)(D+1)(D+4)}, -\frac{1}{2(D^3-3D^2-6D+8)}, \frac{1}{36-9D^2}, \frac{1}{18D+18}, \right. \\
& \left. \frac{1}{18-18D}, -\frac{1}{36(D+4)}, \frac{1}{36(D-4)}, 0 \right\}, \\
\mathbf{v}_{16} = & \left\{ 0, \frac{1}{9D-D^3}, \frac{1}{2(D-2)(D+1)(D+4)}, \frac{1}{2(D^3-3D^2-6D+8)}, -\frac{8-3D^2}{72D-18D^3}, \right. \\
& \left. \frac{D+2}{9(D^2+4D+3)}, \frac{D-2}{9(D-3)(D-1)}, -\frac{1}{36(D+4)}, \frac{1}{144-36D}, 0 \right\}, \\
\mathbf{v}_{17} = & \left\{ \frac{D^4-8D^2+6}{D^6-13D^4+36D^2}, \frac{3-D^2}{D^2(D^2-9)}, -\frac{D(D+3)}{2(D^4+5D^3-20D-16)}, -\frac{(D-3)D}{2(D^4-5D^3+20D-16)}, \right. \\
& \left. \frac{6-4D^2}{36D^2-9D^4}, \frac{2}{9(D+1)(D+3)}, \frac{2}{9(D^2-4D+3)}, \frac{1}{18(D+3)(D+4)}, \frac{1}{18(D^2-7D+12)}, 0 \right\}, \\
\mathbf{v}_{18} = & \left\{ \frac{1}{9D-D^3}, -\frac{1}{18D-2D^3}, -\frac{D}{4(D^3+3D^2-6D-8)}, \frac{D}{4(D^3-3D^2-6D+8)}, -\frac{2}{36D-9D^3}, \right.
\end{aligned}$$

$$\begin{aligned}
& \left. \frac{1}{18(D^2+4D+3)}, -\frac{1}{18(D^2-4D+3)}, \frac{1}{18(D+3)(D+4)}, -\frac{1}{18(D-4)(D-3)}, 0 \right\}, \\
\mathbf{v}_{19} = & \left\{ \frac{1}{9D-D^3}, \frac{2}{D(D^2-9)}, \frac{1}{(D-2)(D+1)(D+4)}, \frac{1}{D^3-3D^2-6D+8}, \frac{4}{36D-9D^3}, \right. \\
& \left. \frac{2}{9(D+1)(D+3)}, -\frac{2}{9(D^2-4D+3)}, \frac{1}{18(D+3)(D+4)}, -\frac{1}{18(D-4)(D-3)}, 0 \right\}, \\
\mathbf{v}_{20} = & \left\{ \frac{2D^2-3}{D^2(D^4-13D^2+36)}, \frac{D^2-3}{2D^2(D^2-9)}, \frac{D^2+3D+4}{-4D^4-20D^3+80D+64}, \right. \\
& \frac{D^2-3D+4}{-4D^4+20D^3-80D+64}, \frac{D^2+3}{9D^2(D^2-4)}, -\frac{1}{9(D+1)(D+3)}, -\frac{1}{9(D^2-4D+3)}, \\
& \left. \frac{1}{18(D+3)(D+4)}, \frac{1}{18(D^2-7D+12)}, 0 \right\}, \\
\mathbf{v}_{21} = & \left\{ \frac{D^2+6}{D^6-13D^4+36D^2}, \frac{3}{D^2(D^2-9)}, \frac{D}{2(D^4+5D^3-20D-16)}, \frac{D}{-2D^4+10D^3-40D+32}, \right. \\
& \left. \frac{D^2-6}{9D^2(D^2-4)}, -\frac{1}{9(D+1)(D+3)}, -\frac{1}{9(D^2-4D+3)}, \frac{1}{18(D+3)(D+4)}, \frac{1}{18(D^2-7D+12)}, 0 \right\}, \\
\mathbf{v}_{22} = & \left\{ \frac{2D^2-3}{D^2(D^4-13D^2+36)}, \frac{3}{18D^2-2D^4}, \frac{3D+4}{4(D^4+5D^3-20D-16)}, \frac{4-3D}{4(D^4-5D^3+20D-16)}, \right. \\
& \left. \frac{3-2D^2}{9D^2(D^2-4)}, \frac{1}{18(D^2+4D+3)}, \frac{1}{18(D^2-4D+3)}, \frac{1}{18(D+3)(D+4)}, \frac{1}{18(D^2-7D+12)}, 0 \right\}, \\
\mathbf{v}_{23} = & \left\{ -\frac{5}{D^5-13D^3+36D}, \frac{1}{9D-D^3}, \frac{D}{2(D^4+5D^3-20D-16)}, \frac{D}{2(D^4-5D^3+20D-16)}, \right. \\
& \left. \frac{1}{36D-9D^3}, -\frac{1}{9(D+1)(D+3)}, \frac{1}{9(D^2-4D+3)}, \frac{1}{18(D+3)(D+4)}, -\frac{1}{18(D-4)(D-3)}, 0 \right\}, \\
\mathbf{v}_{24} = & \left\{ \frac{3}{9D-D^3}, 0, \frac{3}{2(D-2)(D+1)(D+4)}, \frac{3}{2(D^3-3D^2-6D+8)}, \frac{2}{12D-3D^3}, 0, 0, \right. \\
& \left. -\frac{1}{6(D+2)(D+3)(D+4)}, -\frac{1}{6(D^3-9D^2+26D-24)}, \frac{2-D^2}{D^5-5D^3+4D} \right\}, \\
\mathbf{v}_{25} = & \left\{ \frac{5}{D^4-13D^2+36}, 0, \frac{1}{2(D^3+7D^2+14D+8)}, \frac{1}{-2D^3+14D^2-28D+16}, 0, 0, 0, \right. \\
& \left. -\frac{1}{6(D+2)(D+3)(D+4)}, \frac{1}{6(D-4)(D-3)(D-2)}, \frac{1}{D^4-5D^2+4} \right\},
\end{aligned}$$

$$v_{26} = \left\{ -\frac{15}{D^5 - 13D^3 + 36D}, 0, -\frac{3}{D^4 + 5D^3 - 20D - 16}, \frac{3}{D^4 - 5D^3 + 20D - 16}, -\frac{1}{12D - 3D^3}, \right. \\ \left. 0, 0, -\frac{1}{6(D+2)(D+3)(D+4)}, -\frac{1}{6(D^3 - 9D^2 + 26D - 24)}, -\frac{2}{D^5 - 5D^3 + 4D} \right\}.$$

References

- [1] X. Chen and T. Zhou, *Quantum chaos dynamics in long-range power law interaction systems*, *Physical Review B* **100** (Aug., 2019).
- [2] C. Sünderhauf, L. Piroli, X.-L. Qi, N. Schuch, and J. I. Cirac, *Quantum chaos in the brownian syk model with large finite n: Otcos and tripartite information*, *Journal of High Energy Physics* **2019** (Nov., 2019).
- [3] T. Kalsi, A. Romito, and H. Schomerus, *Hierarchical analytical approach to universal spectral correlations in brownian quantum chaos*, 2024.
- [4] L. Brady and V. Sahakian, *Scrambling with matrix black holes*, *Physical Review D* **88** (Aug., 2013).
- [5] P. Pelliconi, J. Sonner, and H. Verlinde, *Gravity as a mesoscopic system*, 2024.
- [6] G. S. Bentsen, S. Sahu, and B. Swingle, *Measurement-induced purification in large-n hybrid brownian circuits*, *Physical Review B* **104** (Sept., 2021).
- [7] Z. Liu and P. Zhang, *Signature of scramblon effective field theory in random spin models*, 2023.
- [8] P. Zhang and Z. Yu, *Dynamical transition of operator size growth in quantum systems embedded in an environment*, *Physical Review Letters* **130** (June, 2023).
- [9] H. Tang, *Brownian Gaussian Unitary Ensemble: non-equilibrium dynamics, efficient k-design and application in classical shadow tomography*, [arXiv:2406.11320](https://arxiv.org/abs/2406.11320).
- [10] P. Saad, S. H. Shenker, and D. Stanford, *A semiclassical ramp in SYK and in gravity*, [arXiv:1806.06840](https://arxiv.org/abs/1806.06840).
- [11] J. Maldacena and D. Stanford, *Remarks on the sachdev-ye-kitaev model*, *Physical Review D* **94** (Nov., 2016).
- [12] J. Maldacena and D. Stanford, *Remarks on the Sachdev-Ye-Kitaev model*, *Phys. Rev. D* **94** (2016), no. 10 106002, [[arXiv:1604.07818](https://arxiv.org/abs/1604.07818)].
- [13] V. Narovlansky and H. Verlinde, *Double-scaled SYK and de Sitter Holography*, [arXiv:2310.16994](https://arxiv.org/abs/2310.16994).
- [14] A. Milekhin and J. Xu, *Revisiting Brownian SYK and its possible relations to de Sitter*, [arXiv:2312.03623](https://arxiv.org/abs/2312.03623).
- [15] D. Stanford, S. Vardhan, and S. Yao, *Scramblon loops*, [arXiv:2311.12121](https://arxiv.org/abs/2311.12121).
- [16] P. Hayden and J. Preskill, *Black holes as mirrors: quantum information in random subsystems*, *Journal of High Energy Physics* **2007** (Sept., 2007) 120–120.
- [17] V. Balasubramanian, A. Kar, C. Li, O. Parrikar, and H. Rajgadia, *Quantum error correction from complexity in Brownian SYK*, *JHEP* **08** (2023) 071, [[arXiv:2301.07108](https://arxiv.org/abs/2301.07108)].

- [18] C. Sünderhauf, L. Piroli, X.-L. Qi, N. Schuch, and J. I. Cirac, *Quantum chaos in the Brownian SYK model with large finite N : OTOCs and tripartite information*, *JHEP* **11** (2019) 038, [[arXiv:1908.00775](#)].
- [19] S.-K. Jian and B. Swingle, *Note on entropy dynamics in the Brownian SYK model*, *JHEP* **03** (2021) 042, [[arXiv:2011.08158](#)].
- [20] L. Agarwal and S. Xu, *Emergent symmetry in Brownian SYK models and charge dependent scrambling*, *JHEP* **22** (2020) 045, [[arXiv:2108.05810](#)].
- [21] D. A. Roberts and B. Yoshida, *Chaos and complexity by design*, *Journal of High Energy Physics* **2017** (Apr., 2017).
- [22] J. Cotler, N. Hunter-Jones, J. Liu, and B. Yoshida, *Chaos, complexity, and random matrices*, *Journal of High Energy Physics* **2017** (Nov., 2017).
- [23] S.-K. Jian, G. Bentsen, and B. Swingle, *Linear growth of circuit complexity from brownian dynamics*, 2022.
- [24] C. Peng, J. Tian, and Y. Yang, *Half-wormholes and ensemble averages*, *Eur. Phys. J. C* **83** (2023), no. 11 993, [[arXiv:2205.01288](#)].
- [25] M. Fava, J. Kurchan, and S. Pappalardi, *Designs via free probability*, 2023.
- [26] C. Dankert, *Efficient simulation of random quantum states and operators*, 2005.
- [27] D. Gross, K. Audenaert, and J. Eisert, *Evenly distributed unitaries: On the structure of unitary designs*, *Journal of Mathematical Physics* **48** (May, 2007).
- [28] A. Ambainis and J. Emerson, *Quantum t -designs: t -wise independence in the quantum world*, 2007.
- [29] C. Dankert, R. Cleve, J. Emerson, and E. Livine, *Exact and approximate unitary 2-designs and their application to fidelity estimation*, *Physical Review A* **80** (July, 2009).
- [30] C.-F. Chen, J. Docter, M. Xu, A. Bouland, and P. Hayden, *Efficient unitary t -designs from random sums*, 2024.
- [31] H. Lin and L. Susskind, *Infinite temperature's not so hot*, 2022.
- [32] C. Dankert, R. Cleve, J. Emerson, and E. Livine, *Exact and approximate unitary 2-designs and their application to fidelity estimation*, *Phys. Rev. A* **80** (Jul, 2009) 012304.
- [33] D. Gross, K. Audenaert, and J. Eisert, *Evenly distributed unitaries: On the structure of unitary designs*, *Journal of Mathematical Physics* **48** (05, 2007) 052104.
- [34] A. Ambainis and J. Emerson, *Quantum t -designs: t -wise independence in the quantum world*, in *Twenty-Second Annual IEEE Conference on Computational Complexity (CCC'07)*, pp. 129–140, 2007.
- [35] A. J. Scott, *Optimizing quantum process tomography with unitary 2-designs*, *Journal of Physics A: Mathematical and Theoretical* **41** (jan, 2008) 055308.
- [36] A. Roy and A. J. Scott, *Unitary designs and codes*, *Designs, Codes and Cryptography* **53** (Apr., 2009) 13–31.
- [37] A. W. Harrow and R. A. Low, *Random quantum circuits are approximate 2-designs*, *Communications in Mathematical Physics* **291** (July, 2009) 257–302.

- [38] F. G. S. L. Brandão, A. W. Harrow, and M. Horodecki, *Local random quantum circuits are approximate polynomial-designs*, *Communications in Mathematical Physics* **346** (Aug., 2016) 397–434.
- [39] Y. Nakata, C. Hirche, M. Koashi, and A. Winter, *Efficient quantum pseudorandomness with nearly time-independent hamiltonian dynamics*, *Physical Review X* **7** (Apr., 2017).
- [40] N. Hunter-Jones, *Unitary designs from statistical mechanics in random quantum circuits*, 2019.
- [41] S. Aaronson, *Shadow tomography of quantum states*, *SIAM J. Comput.* **49** (2020), no. 5 STOC18–368–STOC18–394, [[arXiv:1711.01053](#)].
- [42] F. M. Haehl and M. Rozali, *Fine Grained Chaos in AdS₂ Gravity*, *Phys. Rev. Lett.* **120** (2018), no. 12 121601, [[arXiv:1712.04963](#)].
- [43] S. Guo, M. Sasieta, and B. Swingle, *Complexity is not Enough for Randomness*, *SciPost Phys.* **17** (2024) 151, [[arXiv:2405.17546](#)].
- [44] M. Hamermesh and A. A. Mullin, *Group theory and its applications to physical problems*, *American Journal of Physics* **30** (1962) 774–775.
- [45] A. Nahum, J. Ruhman, S. Vijay, and J. Haah, *Quantum entanglement growth under random unitary dynamics*, *Physical Review X* **7** (July, 2017).
- [46] A. Nahum, S. Vijay, and J. Haah, *Operator spreading in random unitary circuits*, *Physical Review X* **8** (Apr., 2018).
- [47] C. von Keyserlingk, T. Rakovszky, F. Pollmann, and S. Sondhi, *Operator hydrodynamics, otocs, and entanglement growth in systems without conservation laws*, *Physical Review X* **8** (2018), no. 2.
- [48] T. Zhou and A. Nahum, *Entanglement membrane in chaotic many-body systems*, *Physical Review X* **10** (Sept., 2020).
- [49] M. P. Fisher, V. Khemani, A. Nahum, and S. Vijay, *Random quantum circuits*, *Annual Review of Condensed Matter Physics* **14** (Mar., 2023) 335–379.
- [50] P. Hayden, S. Nezami, X.-L. Qi, N. Thomas, M. Walter, and Z. Yang, *Holographic duality from random tensor networks*, *Journal of High Energy Physics* **2016** (Nov., 2016).
- [51] P. Hosur, X.-L. Qi, D. A. Roberts, and B. Yoshida, *Chaos in quantum channels*, *JHEP* **02** (2016) 004, [[arXiv:1511.04021](#)].
- [52] J. Maldacena, *Eternal black holes in anti-de sitter*, *Journal of High Energy Physics* **2003** (Apr., 2003) 021–021.
- [53] P. Saad, *Late time correlation functions, baby universes, and eth in jt gravity*, 2019.
- [54] D. Stanford, *More quantum noise from wormholes*, 2020.
- [55] C. Peng, J. Tian, and J. Yu, *Baby universes, ensemble averages and factorizations with matters*, [arXiv:2111.14856](#).